Dear Prof. Grothe,

Two referees, referred to below as Referee #2 and Referee #3 based on the manuscript submission records, reviewed this manuscript (Referee #1 did not submit a review). Dr. Douglas Day and several researchers from the research group of Prof. Jose Jimenez kindly contributed additional comments. Our final response contains responses to seven comments from Reviewer 2, six comments from Reviewer 3, and fifteen comments from Dr. Day. Thank you for considering our manuscript for publication in Atmospheric Chemistry and Physics. We also express our gratitude to the referees and to members of Prof. Jimenez' research group; in our opinion, their collective input has led to a significantly improved manuscript.

Best regards,
Andrew Lambe

Referee #2 comments

1) Since the authors do not really discuss oxidation mechanisms in detail, it is not necessary for this manuscript to show the various SOA precursors in Figure 1. I recommend removing Figure 1 and adjusting section 2.2 accordingly, just mentioning the precursors in the text.

Response. Per the referee's suggestion we removed Figure 1 from the manuscript. We revised the text in Section 2.2 as follows (changes in bold and strikethrough):

P30582, L1-5: "~~Figure 1 shows~~ **T**he gas-phase SOA precursors used in these studies **include** two biogenic gases (isoprene, α-pinene), three aromatic compounds (toluene, *m*-xylene, naphthalene), and three alkanes (*n*-C_{10}, cyclodecane, tricyclo[5.2.1.$0^{2,6}$]decane, also known as JP10)."

2) In section 3.1, the SOA mass spectra generated from alpha-pinene and naphthalene in an environmental chamber and a flow reactor are compared. It is stated that the chamber and flow reactor mass spectra are similar. What is the measure of similarity used for this statement? Did the authors use a quantitative measure for comparing mass spectra, e.g. a cluster analysis approach? What exactly are the SOA signal data shown in the insets of Figure 2c and d? Are these the sum signal of the AMS data? Please extend the comparison of the mass spectra and the explanation of the derived SOA signal!

Response. In the discussions manuscript, we used the linear regression parameters to conclude that the spectra are similar (slope = 0.91-0.92, r^2 = 0.93-0.94). These parameters are shown in the insets of Figure 2c and d. We assume the referee views these as insufficient measures of similarity between the mass spectra, and that the referee is additionally suggesting using a cluster analysis as a quantitative measure of similarity. To address this comment we applied a methodology similar to that of Murphy et al. (2003) and Marcolli et al. (2006). These studies calculated the dot product of two normalized mass spectra as a measure of similarity; a dot product of zero indicates the mass spectra are orthogonal and a dot product of one indicates the mass spectra are identical. Using this approach we calculated dot products between SOA mass spectra generated from α-pinene and naphthalene respectively in the Caltech environmental chamber and the PAM flow reactor.

The SOA signal data shown in the Figure 2c inset is a scatter plot of the α-pinene SOA mass spectra shown in Figures 2a and c. Likewise, the Figure 2d inset is a scatter plot of the naphthalene SOA mass spectra shown in Figure 2b and d. We apologize that this was unclear. In an attempt address the referee's request for an extended comparison of the mass spectra, we added two tables to Figure 2 showing dot products and correlation coefficients between six pairs of mass spectra: Figures 2a and b, 2a and c, 2a and d, 2b and c, 2b and d, and 2c and d. With these revisions, the scatter plots that were originally shown as figure insets are no longer necessary and have removed them from the figure. Revisions to the Section 3.1 discussion and Figure 2 are shown below (changes bolded).

P30584, L3-L22: "Figure 2 shows representative ToF-AMS spectra of SOA generated in the PAM reactor and the Caltech chamber (Chhabra et al., 2010, 2011) from the OH oxidation of *α*-pinene and naphthalene […] In this range the OH exposure for the PAM reactor and chamber are approximately the same, allowing for direct comparison.

To quantify the similarity between mass spectra, we calculated the dot product between SOA mass spectra generated in the PAM flow reactor and the Caltech chamber (Murphy et al., 2003, Marcolli et al., 2006). Using this approach, each mass spectral signal is normalized to the square root of the sum of the squares of all signals in the mass spectrum. Each spectrum is represented as a normalized vector A or B, with dot product $\boldsymbol{A \cdot B = \sum_{i=1}^{n} a_i b_i}$, where a_i and b_i are the normalized signals at each *m/z* in the spectrum; $\boldsymbol{A \cdot B = 0}$ indicates the spectra are orthogonal and $\boldsymbol{A \cdot B = 1}$ indicates the spectra are identical.

The top table inset in Figure 2 shows the calculated dot products between each pair of mass spectra. The PAM flow reactor and the chamber produce particles with similar mass spectra, as indicated by dot products of 0.97 between spectra shown in Figs. 2a and c (α-pinene SOA) and Figs. 2b and d (naphthalene SOA), suggesting similar compositions. Features unique to *α*-pinene and naphthalene SOA are observed in both flow reactor- and chamber-obtained spectra, with linear correlation coefficients of r^2 = 0.93 (*α*-pinene SOA) and r^2 = 0.94 (naphthalene SOA) as noted **in the bottom table inset** in Fig. 2. […] As is evident from Fig. 2, *α*-pinene and naphthalene SOA mass spectra display pronounced differences, **with dot products ranging from 0.42 to 0.63 and** r^2 **ranging from** 0.**18 to 0.37** between spectra shown in Figs. 2a and b, 2a and d, 2b and c, and 2c and d.

We added the following citations for Murphy et al. (2003) and Marcolli et al. (2006) to the listed References:

D. M. Murphy, A. M. Middlebrook & M. Warshawsky. Cluster Analysis of Data from the Particle Analysis by Laser Mass Spectrometry (PALMS) Instrument, Aerosol Science and Technology, 37:4, 382-391, DOI: 10.1080/02786820300971, 2003.

C. Marcolli, M. R. Canagaratna, D. R. Worsnop, R. Bahreini, J. A. de Gouw, C. Warneke, P. D. Goldan, W. C. Kuster, E. J. Williams, B. M. Lerner, J. M. Roberts, J. F. Meagher, F. C. Fehsenfeld, M. Marchewka, S. B. Bertman, and A. M. Middlebrook. Cluster Analysis of the Organic Peaks in Bulk Mass Spectra Obtained During the 2002 New England Air Quality Study with an Aerodyne Aerosol Mass Spectrometer. Atmos. Chem. Phys., 6, 5649–5666, 2006.

We revised Figure 2 (Figure 1 in revised manuscript) as shown below:

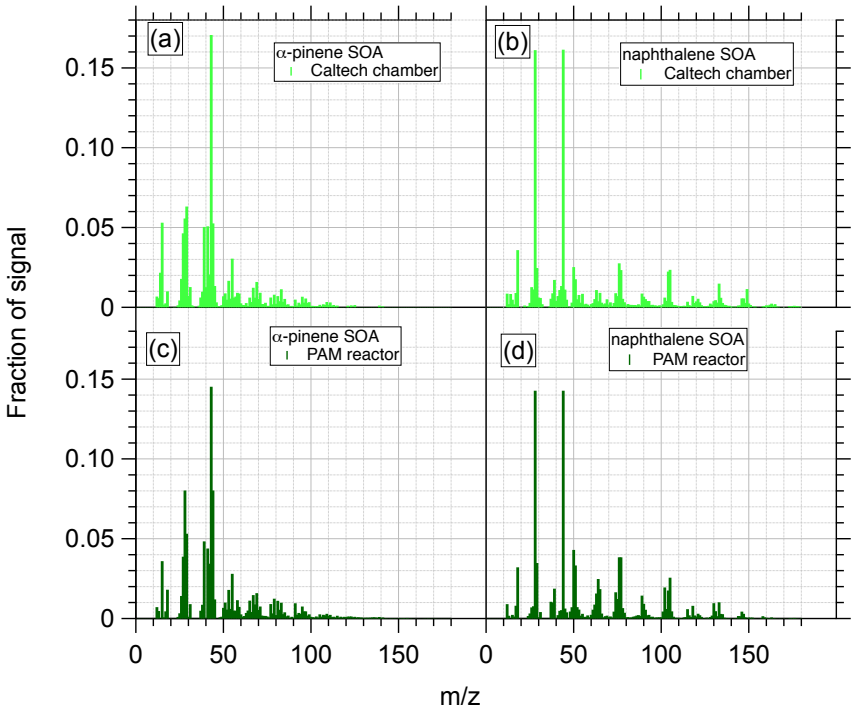

Dot Product Between Mass Spectra

	a	b	c	d
a	1	0.46	**0.97**	0.42
b	-	1	0.63	**0.97**
c	-	-	1	0.59
d	-	-	-	1

Linear Correlation Coefficient (r^2) Between Mass Spectra

	a	b	c	d
a	1	0.18	**0.93**	0.15
b	-	1	0.37	**0.94**
c	-	-	1	0.32
d	-	-	-	1

3) I do not agree with the interpretation of Figure 4 in section 3.3! The authors state that their results show that the chambers and the flow reactor provide similar average carbon oxidation states for a specific SOA type over the range of measured SOA composition for comparable OH exposures. They justify this statement by noting that the observed deviations between the flow reactor and the chambers are no larger than deviations between two chambers. From this, the only conclusion I can draw is that for various types of SOA there is no preference for a flow reactor or a chamber experiment. However, the average carbon oxidation states obtained from experiments with different setups may vary substantially. They are not always similar! Please clarify your statement.

Response. We assume the referee is referring to the following subset of SOA types where the absolute differences in OSc between flow reactor and chamber are larger than in most other cases:

toluene SOA: OSc = -0.05 (Caltech), 0.55 (PAM)
cyclodecane SOA: OSc = -0.74 (CMU), -0.38 (PAM), 0.03 (MIT)
α-Pinene SOA: OSc = -0.53 (PAM), 0.04 (PSI)

In this context, we assume the referee does not agree with the following statement on P30586, L15-16: "Figure 4 shows that the chambers and flow reactor provide similar OSc for a specific SOA type over the range of measured SOA composition for comparable OH exposures." In an attempt to address the referee's concern we revised this sentence as shown below:

P30586, L15-16: "**For a specific SOA type,** Figure 4 shows that the chambers and flow reactor provide ~~similar~~ OSc ~~for a specific SOA type~~ **with absolute differences ranging from 0.0040 to**

0.60 (average deviation = 0.10 ± 0.34) over the range of measured SOA composition for comparable OH exposures."

4) In section 3.4 (page 30587, lines 3/4) it is stated again that mass spectra and elemental ratios of SOA from flow reactor and chamber experiments are similar. What is the used measure of similarity for mass spectra?

Response. Please see our response to Comment #2 above, where we note that we used linear regression fit parameters (and, in the revised manuscript, dot products) between SOA mass spectra generated in the PAM flow reactor and Caltech environmental chamber as measures of similarity. In attempt to clarify this point, we revised the text as follows to refer the reader back to Section 3.1:

P30587, L3-4: "Because mass spectra and elemental ratios of SOA are similar whether it is generated in an environmental chamber or in a flow reactor **(Section 3.1)**…"

5) **P30587, lines 21/22**: It is not evident to me from Figure 5 that SOA yields at comparable OH exposures are a factor of 2 to 10 lower in the flow reactor than in chambers. Given the strong dependence of alpha-pinene SOA yields on OH exposure shown in Fig. 5b, I cannot compare any data points in Fig. 5a. In Fig. 5b, there are no large differences between flow reactor and chamber data points. Fig. 5c may suggest a lower SOA yield by a factor of about 5 in the flow reactor, but given the large uncertainties of the yield estimates, I think a quantitative interpretation of Figure 5 is not adequate. Please clarify this passage.

Response. This is a fair point (see also related Comment # 5 by Douglas Day). We assume that the referee agrees that yields are systematically lower in the flow reactor than in the chambers. We have revised the text as follows (changes in strikethrough:

6) **P30587, L21-22**: "1. SOA yields at comparable OH exposures are ~~a factor of 2 to 10~~ lower in the flow reactor than in chambers, whereas the mass spectra, O/C and H/C of SOA generated in the chambers and flow reactor are similar (Figs. 2–4)."

7) **Technical comments page 30583, line 20**: remove "degree" in "-0.02 per degree K" page 30589, line 27: replace "concentrations" by "concentration"

Response. Thank you for pointing these out. We made the suggested changes.

Referee #3 comments

1) Title: The title is extensively long and appears to be more a short abstract then a title. I recommend shortening of the title in a focusing form.

Response. Per the referee's suggestion we will change the title from "Comparison of secondary organic aerosol formed with an aerosol flow reactor and environmental reaction chambers: effect of oxidant concentration, exposure time and seed particles on chemical composition and yield" to "Effect of oxidant concentration, exposure time and seed particles on secondary organic aerosol chemical composition and yield"

2) Introduction: The introduction well introduces the reader to the scientific content of the present work. However, present intercomparison studies are not discussed. The discussion of the comparability of these two experimental setups is of highest interest for the community and should therefore be introduced as well. For example: Jang et al. (Environ. Sci. Technol. 2003, 37, 3828-3837, doi: 10.1021/es021005u) studied the aerosol growth by heterogeneous nucleation on seed particles in a flow reactor and an aerosol chamber. Ofner et al. (Z. Phys. Chem., 2010, 224, 1171-1183, doi: 10.1524.zpch.2010.6146) studied and compared the evolution of infrared active func- tional groups using a flow reactor and a smog chamber. The evolution of carbonyls in this study can be linked to the averaged carbon oxidation state. Bernhard et al. (J. Aerosol Sci., 2012, 43, 14-30, doi: 10.1016/j.jaerosci.2011.08.005) compared the ozonisation of mono-terpenes in a flow-reactor with aerosol chamber studies. Further, the cited studies on flow reactor measurements should be discussed in more detail.

Response. Thank you for bringing these studies to our attention. We have revised text in the Introduction as follows:

P30579-P30580, L29-6: "A growing set of studies […] (Bahreini et al., 2012; Lambe et al., 2012, 2011b; Kang et al., 2011; Massoli et al., 2010; Ortega et al., 2013; Slowik et al., 2012; Wang et al., 2012; Wong et al., 2011). **Other studies have used a combination of aerosol flow reactors and environmental chambers to characterize heterogeneous uptake of organics on seed particles (Jang et al., 2003), SOA formation potential (Kang et al., 2007; Bernard et al., 2012), and evolution of functional groups in SOA with aging (Ofner et al., 2010); in general, similar results are obtained in reactors and chambers.** However, these comparisons need to be extended over a wider range of reactants and experimental conditions than are currently available."

We added the following citations to References:

Jang, M., B. Carroll, B. Chandramouli, and R. M. Kamens, Particle Growth By Acid-Catalyzed Heterogeneous Reactions of Organic Carbonyls on Preexisting Aersols, *Environ. Sci. Technol*., 37, 3828-3837, 2003**.**

Ofner, J., H.-U. Krüger, and C. Zetzsch, Time Resolved Infrared Spectroscopy of Formation and Processing of Secondary Organic Aerosol, *Z. Phys. Chem*., 224, 1171–1183, 2010, DOI:10.1524.zpch.2010.6146.

Bernard, F., I. Fedioun, F. Peyroux, A. Quilgars, V. Daële, A. Mellouki, Thresholds of secondary organic aerosol formation by ozonolysis of monoterpenes measured in a laminar flow aerosol reactor, *Journal of Aerosol Science*, 43, 14—30, 2012.

3) Experimental: The experimental setup of the PAM reactor should be reported in more detail. While the involved aerosol chambers are well defined in the literature, only rudimentary information on the PAM reactor is provided. Especially, UV/VIS spectra of the applied mercury lamps, which cause photolysis inside the flow reactor, and photon flux measurements would be interesting. The knowledge of the photon flux inside the reactor would assist the calculation of photolysis rates of several gaseous species.

Response. We have added text (changes bolded) to the Experimental section to describe UV/Vis spectra of the mercury lamps and photolysis flux calculations inside the reactor.

P30581, L4-L13: "In the flow reactor, OH radicals were produced in the absence of NO_x via the reaction $O(^1D) + H_2O \rightarrow 2OH$, with $O(^1D)$ radicals produced from the reaction $O_3 + h\nu \rightarrow O_2 + O(^1D)$. O_3 was generated by O_2 irradiation with a mercury lamp (λ = 185 nm) outside the flow reactor. The $O(^1D)$ atoms were produced by UV photolysis of O_3 inside the flow reactor using four mercury lamps **which emit primarily at λ = 254 nm. Additional photons are emitted at the following wavelengths with relative intensities of 1% or more of the UV intensity at 254 nm: 185 nm (~1%; Li et al., 2015); 302 nm (1%); 313 nm (1%) 366 nm (1%); 405 nm (1%); 436 nm (10%); 546 nm (1%) (BHK Inc. Analamp product technical specifications)** […]. The corresponding OH exposures ranged from 2.0×10^{10} to 2.2×10^{12} molec cm^{-3} s or approximately 0.2 to 17 days of equivalent atmospheric exposure.

At the highest UV intensity that was used in the reactor, we calculate upper-bound J_{UV} = 2×10^{13} and 2×10^{15} cm^{-2} s^{-1} at λ = 185 and 254 nm from ozone and OH exposure measurements. Corresponding lower limit timescales for UV photolysis of several phenols, carboxylic acids, aldehydes and ketones range from 12 to 50,000 sec for absorption cross sections ranging from approximately 4×10^{-17} to 1×10^{-20} cm^3 $molec^{-1}$ s^{-1} (https://sites.google.com/site/pamwiki/; and references therein)."

Below is the UV-Vis emission spectrum of the lamps provided on the manufacturer website:

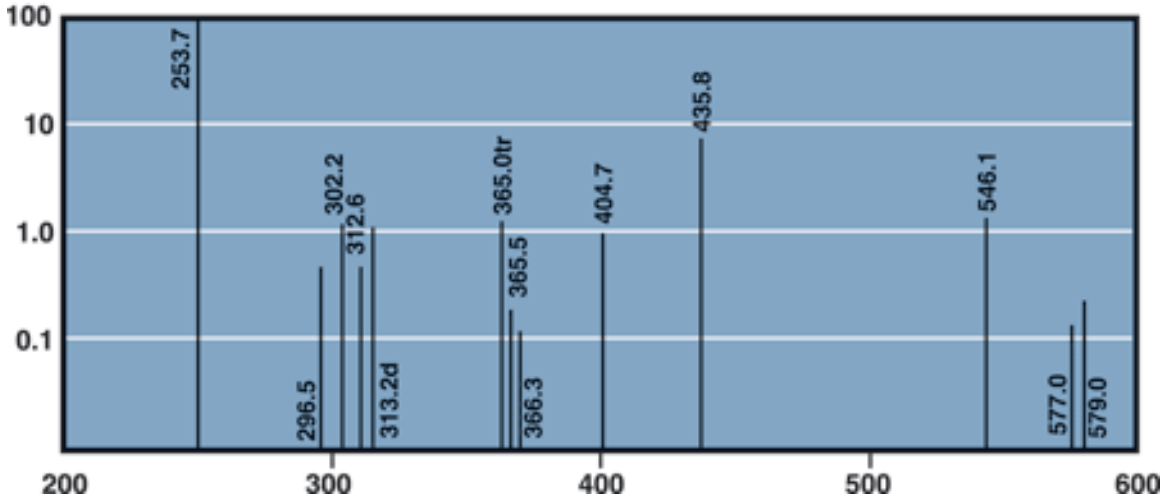

The following citation has been added to References:

R. Li, W.H. Brune, B.B. Palm, A.M. Ortega, J. Hlywiak, W. Hu, Z. Peng, D.A. Day, C. Knote, J. de Gouw, and J. L. Jimenez. Modeling the radical chemistry in an Oxidation Flow Reactor: radical formation and recycling, sensitivities, and OH exposure calibration equation. *Journal of Physical Chemistry A*, 2015, submitted.

4) Particle monitoring and analysis – p. 30582, line 24ff "While AMS measurements . . . additional supporting measurements . . .": Please specify these supporting measurements. Several other techniques, especially optical spectroscopy in the UV/VIS and IR is able to assist AMS

measurements. Also offline techniques like FT/MS could assist the interpretation of chemical reactions related to aerosol formation in aerosol chamber and aerosol flow reactor beyond O/C ratios and the averaged carbon oxidation state.

Response. We have revised the text as follows (changes bolded):

P30582, L24: "While AMS measurements provide basic information about SOA composition, additional supporting measurements **such as Fourier transform infrared spectroscopy, nuclear magnetic resonance, gas chromatography – mass spectrometry, and chemical ionization mass spectrometry** are required to investigate SOA chemistry at the molecular level."

5) **p. 30585, l. 17**: "The observation suggests . . ." This sentence is of utmost importance due to the discussion of comparability of these two methods and should therefore be discussed in detail and added to the abstract and the results.

Response. We revised the abstract as follows (changes marked in bold and strike-through).

P30577: "The OH concentration in the chamber experiments is close to that found in the atmosphere, but the integrated OH exposure in the flow reactor can simulate atmospheric exposure times of multiple days compared to chamber exposure times of only a day or so. **In most cases, for a specific SOA type the most-oxidized chamber SOA and the least-oxidized flow reactor SOA have similar mass spectra, oxygen-to-carbon and hydrogen-to-carbon ratios, and carbon oxidation states at integrated OH exposures between approximately 1 × 10^{11} and 2 × 10^{11} molec cm^{-3} s, or about 1–2 days of equivalent atmospheric oxidation. This observation suggests that in the range of available OH exposure overlap for the flow reactor and chambers, SOA elemental composition as measured by an aerosol mass spectrometer is similar whether the precursor is exposed to low OH concentrations over long exposure times or high OH concentrations over short exposures times.** ~~A linear correlation analysis of the mass spectra (m = 0.91–0.92, r^2 = 0.93–0.94) and carbon oxidation state (m = 1.1, r^2 = 0.58) of SOA produced in the flow reactor and environmental chambers for OH exposures of approximately 10^{11} molec cm^{-3} s suggests that the composition of SOA produced in the flow reactor and chambers is the same within experimental accuracy as measured with an aerosol mass spectrometer.~~ This similarity in turn suggests that both in the flow reactor and in chambers, SOA chemical composition at low OH exposure is governed primarily by gas-phase OH oxidation of the precursors, rather than heterogeneous oxidation of the condensed particles. In general, SOA yields measured in the flow reactor are lower than measured in chambers for the range of equivalent OH exposures that can be measured in both the flow reactor and chambers. The influence of sulfate seed particles on isoprene SOA yield measurements was examined in the flow reactor. The studies show that seed particles increase the yield of SOA produced in flow reactors by a factor of 3 to 5 and may also account in part for higher SOA yields obtained in the chambers, where seed particles are routinely used."

In addition to the above text located on P30585, L17, similar statements are mentioned and discussed in the following locations of the discussions manuscript:

P30584, L11-L12 (Section 3.1): "The PAM flow reactor and the chamber produce particles with similar mass spectra, suggesting similar compositions."

P30586, L14-L16 (Section 3.3): "Figure 4 shows that the chambers and flow reactor provide similar OSc for a specific SOA type over the range of measured SOA composition for comparable OH exposures."

P30590, L20-L22: (Section 4): "Within the range of approximate OH exposure overlap of (1–4) $\times 10^{11}$ molec cm^{-3} s, the SOA mass spectra and oxidation state were similar in both systems."

In our opinion, after revising the abstract in accordance with the referee's suggestion, this topic is now sufficiently expressed in the revised manuscript.

6) Figure 7 (and some others as well): If the 1 sigma uncertainty is in the size range of the symbol, please remove the error bars to prevent misinterpretation of the kind of symbol.

Response. We assume the referee is referring primarily to Figure 3 in addition to Figure 7. Figures 3 and 7 have been revised as shown below (left = figure in discussions manuscript; right = figure in revised manuscript):

FIGURE 3

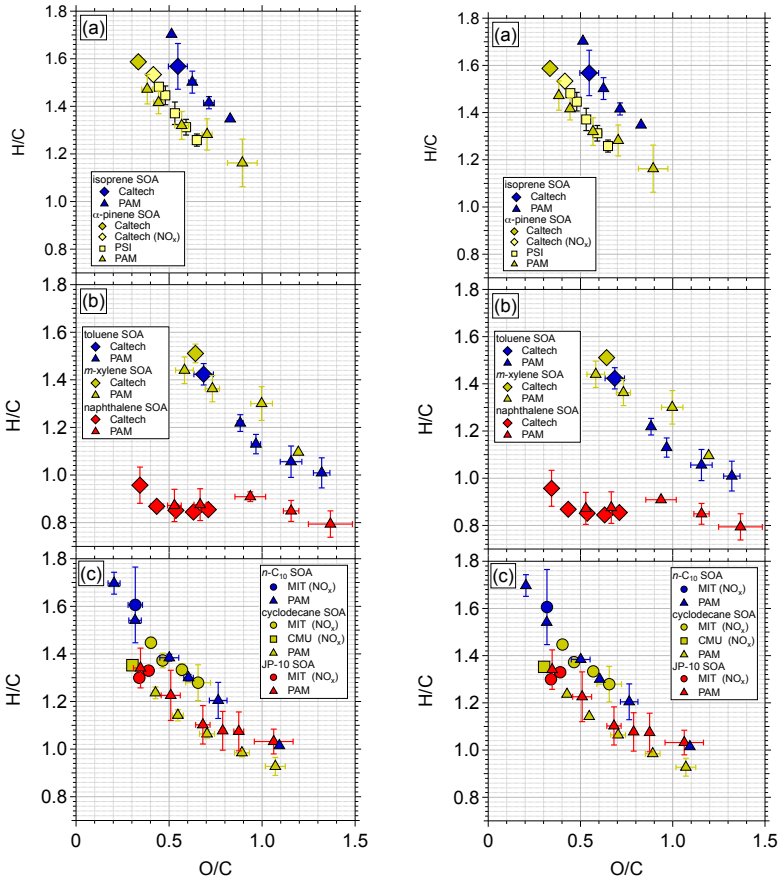

FIGURE 7

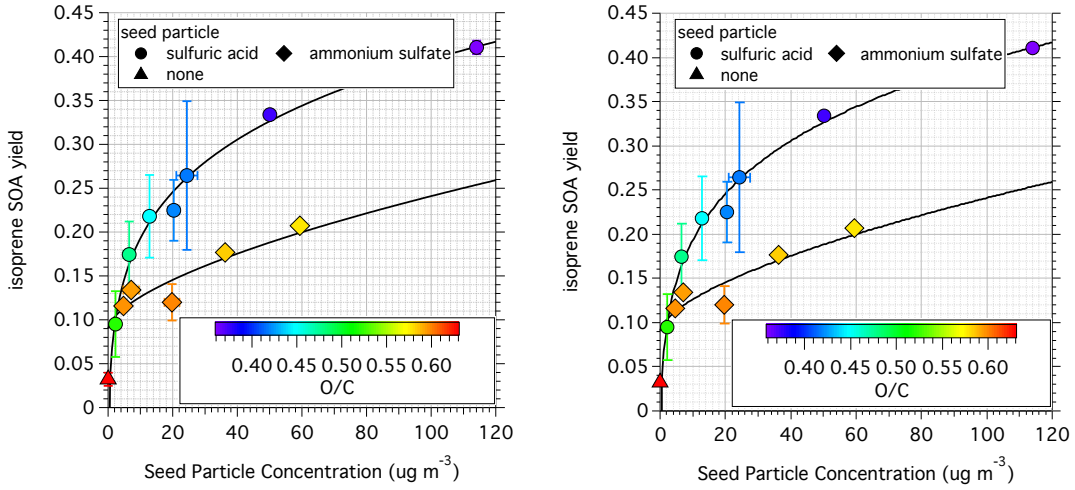

Douglas Day comments

1) One critical aspect, in particular, is the lack of information on how the OH exposure (OH_{exp}) is calculated. The only reference to OH_{exp} calculations appears in Sect. 2.1 (p 30581, lines 8-13) as "OH concentrations were varied by changing the UV light intensity, and were quantified by measuring the decay of SO_2 and applying the known OH+ SO_2 rate constant (Davis et al., 1979)." Depending on the details of how such experiments were done, there could be substantial errors in the estimated OH_{exp}. However there is not sufficient detail in the manuscript to ascertain whether this is the case or not. It would be very useful to the community and the future users of the results of this paper if more details were provided, so readers and other researchers don't have to speculate whether disagreements may be due to errors or uncertainties in OH_{exp}.

2) As discussed in Ortega et al. (2013) and Li et al. (2015), high VOC concentrations (or high concentrations of other compounds that react with OH) can "suppress" OH by shifting OH to HO_2 in the reactor, resulting in much lower OH exposures than measured for the same conditions in the absence of added "external OH reactivity" (OHR_{ext}). Measurements and modeling carried out by our group (using reactors that employ either 254 nm only or both 254 + 185 nm wavelengths from mercury lamps to generate OH) suggests this "OH suppression" can reach 1-2 orders-of-magnitude for high OHR_{ext} (100-1000 s^{-1}). Very high OHR_{ext} were indeed used in the experiments described in this paper. With the information provided, it is impossible to know if the effects of OH suppression from high OHR_{ext} were accounted for or not in this study. Several critical pieces of information include:

- Were the SO_2 decay measurements performed only "offline", i.e. in the absence of VOC? Or were they carried out "online" (in the presence of added VOC)?
- If offline, at what range of OHR_{ext} (i.e. SO_2 concentrations)?
- What H_2O concentrations were used for the calibrations and how do they compare to those used in the VOC experiments, if those were different experiments?

- What input O_3 levels were used for the SO_2 and VOC experiments?
- Were the calibrations and SOA experiments conducted close in time? Hg lamps age with time and the same light power setting may not correspond to the same UV flux if multiple months have passed.

Response. We have revised the text shown below (changes in response to Comment #1 are shown in bold/strikethrough; changes in response to Comment #2 are shown in red).

P30581, L4-10: "In the flow reactor, OH radicals were produced in the absence of NO_x via the reaction $O(^1D) + H_2O \rightarrow 2OH$, with $O(^1D)$ radicals produced from the reaction $O_3 + h\nu \rightarrow O_2 + O(^1D)$. O_3 (15 – 30 ppm) was generated by O_2 irradiation with a mercury lamp (λ = 185 nm) outside the flow reactor. The $O(^1D)$ atoms were produced by UV photolysis of O_3 inside the flow reactor using four mercury lamps (λ = 254 nm). In offline calibrations, OH concentrations were varied by changing the UV light intensity **through stepping the lamp voltages between 0 and 110V**. SO_2 was added to the carrier gas, typically at mixing ratios ranging from 30 to 60 ppbv, and was used as an OH tracer. Calibrations were conducted at the same H_2O and O_3 concentrations used in SOA experiments.

At each lamp setting, OH exposures were quantified by measuring the steady-state SO_2 mixing ratio and normalizing to the SO_2 mixing ratio obtained with the lamps turned off. The corresponding OH exposure (OH_{exp}) was quantified by ~~measuring the decay of SO_2~~ **normalizing the SO_2 mixing ratio with the lamps on to the SO_2 mixing ratio with the lamps off** and applying the known OH+SO_2 rate constant, $\boldsymbol{k_{SO_2}^{OH}}$, (Davis et al., 1979)**, as shown in Equation 1:**

$$\boldsymbol{OH_{exp} = -\frac{1}{k_{SO_2}^{OH}} ln\left(\frac{[SO_2]}{[SO_2]_i}\right)}$$

The concentrations ranged from approximately 2.0×10^8 to 2.2×10^{10} molec cm^{-3}. The corresponding OH exposures ranged from 2.0×10^{10} to 2.2×10^{12} molec cm^{-3} s or approximately 0.2 to 17 days of equivalent atmospheric exposure.

Additional SO_2 calibration measurements were conducted in the presence and absence of a subset of precursors (isoprene and JP-10) to investigate reductions in OH levels following addition of those precursors to the flow reactor at mixing ratios that were used in SOA experiments. No change in SO_2 decay was observed upon addition of isoprene, but addition of JP-10 decreased OH levels by approximately 10% (highest OH exposure) to 50% (lowest OH exposure) (Lambe et al., 2012). Reductions in OH exposure following addition of other VOCs will be investigated in future work using the methods of Li et al. (2015).

P30607, Figure 5 caption: "Yields of SOA produced from photoxidation of **(a)** isoprene, **(b)** α-pinene, and **(c)** tetracyclo[5.2.1.$0^{2,6}$]decane (JP-10) in environmental chambers and PAM reactor as a function of OH exposure. The OH exposure in Fig. 5c is corrected for reductions in OH levels upon JP-10 addition (see Section 2.1)."

3) H_2O and O_3 concentrations will strongly affect both OH_{exp} and degree of OH suppression for a given lamp setting. If calibrations were not conducted at relevant conditions or characterization of the effects of OH suppression estimated, a discussion of possible biases should be included in the manuscript, or (better) OH_{exp} calibration experiments should be conducted under conditions

representative of the OHR_{ext} of the experiments. If differences in OH suppression between calibrations and VOC experiments were corrected for, the details of such corrections should be thoroughly described in the paper.

Response. OH exposure calibrations were conducted at the same H_2O and O_3 concentrations that were used during SOA formation experiments. In the present work, calibrated OH exposure data are shown for in Figure 5 for isoprene SOA, α-pinene SOA, and JP-10 SOA formation experiments. We conducted OH exposure calibrations in the presence and absence of isoprene (added at 462 ppbv mixing ratio) and did not observe changes in OH exposure upon isoprene addition, so no correction was applied. We have not measured OH exposure reductions upon addition of α-pinene. As suggested by Li et al. (2015), we will conduct OH exposure calibrations in the presence of α-pinene (and othere relevant VOCs) in future work. We conducted OH exposure calibrations in the presence and absence of JP-10 (added at 55 ppbv mixing ratio). A 10%-50% reduction in OH exposure was observed upon addition of 55 ppb JP-10; we initially reported this result in Lambe et al. (2012). Results shown in Figure 5c of the discussions manuscript accounted for this reduction in OH exposure and the revised manuscript mentions this correction.

4) Also, for conditions with high VOC concentrations, RO_2+SO_2 reactions may cause substantial decay in SO_2, not attributable to OH (Kan et al., 1981; Richards-Henderson et al., 2014). Therefore, if online calibrations were conducted (i.e. if the SO_2 was introduced at the same time as the VOC) this may cause a substantial overestimate in OH_{exp}. If additional high OHR_{ext} calibrations/characterizations experiments are conducted, use of an additional compound that reacts with OH but not RO_2, such as CO, would help eliminate errors arising from that cause.

Response. The Kan et al. (1981) study measured a bimolecular reaction rate constant k_{RO2}^{SO2} = $1.4*10^{-14}$ cm^3 s^{-1} between SO_2 and methylperoxy (CH_3O_2) radicals. However, other studies have measured much slower SO_2 + RO_2 reaction kinetics. Sander and Watson (1981) reported an upper limit reaction rate $k_{RO2}^{SO2} < 5*10^{-17}$ cm^3 s^{-1}, a value that is more than 100 times lower than Kan et al. (1981). A computational study by Kurten et al. (2011) suggests an even lower upper-bound reaction rate constant $k_{RO2}^{SO2} < 5*10^{-21}$ cm^3 s^{-1}. JPL Evaluation 17 (2011) recommends the Sander and Watson result, as summarized below, with a possible experimental artifact in the Kan et al. (1981) result highlighted:

> *"This recommendation accepts the results from the study of Sander and Watson [1255]. These authors conducted experiments using much lower CH_3O_2 concentrations than employed in the earlier investigations of Sanhueza et al. [1259] and Kan et al. [765], both of which resulted in k(298 K) values approximately 100 times greater. A later report by Kan et al. [764] postulates that these differences are due to the reactive removal of the $CH_3O_2SO_2$ adduct at high CH_3O_2 concentrations prior to its reversible decomposition into CH_3O_2 and SO_2. They suggest that such behavior of $CH_3O_2SO_2$ or its equilibrated adduct with O2 ($CH_3O_2SO_2O_2$) would be expected in the studies yielding high k values, while decomposition of $CH_3O_2SO_2$ into reactants would dominate in the Sander and Watson experiments. It does not appear likely that such secondary reactions involving CH_3O_2, NO, or other radical species would be rapid enough, if they occur under normal atmospheric conditions to compete with the adduct decomposition."*

We simulated PAM reactor photochemistry over a range of conditions that are representative of

the SOA formation experiments used in this work. The photochemical box model was developed by W. H. Brune and is a revised version of the model described in Li et al. (2015) that incorporates additional RO_2 + SO_2 reactions following the oxidation of added VOCs to form RO_2 radicals. The following inputs were used in the model:

Mean residence time = 100 sec
Flux254 (cm^{-2} s^{-1})= [2e14; 4e14; 6e14; 8e14; 1e15; 2e15]
Flux254 (cm^{-2} s^{-1})= [2e12; 4e12; 6e12; 8e12; 1e13; 2e13]
$[O_3]_i$ = 20 ppmv
$[H_2O]$ = 1.1 %
$[SO_2]_i$ = 60 ppbv
$[VOC]_i$ (ppbv) = [10; 100; 500]
k_OH_VOC = 10e-11 (cm^3 s^{-1})
k_ro2_so2 = 1.4e-14 cm^3 s^{-1} [Case 1; Kan et al. (1981)]
k_ro2_so2 = 5e-17 cm^3 s^{-1} [Case 2; Sander and Walker (1981)]

The above range of UV intensities covers most of the experimental conditions used in our measurements. This range of conditions corresponds to "external" OH reactivities (OHR_{ext}) of 24.6, 246, and 1230 s^{-1}, respectively, which span the range of OHR_{ext} for data presented in Table 2 and Figures 5-7. For example, the addition of 55 ppb JP-10 is equivalent to OHR_{ext} ~ 31 s^{-1} assuming k_OH_VOC = 2.3*10^{-11} cm^3 s^{-1} (Lambe et al., 2012 supporting information). The addition of 41 to 100 ppb α-pinene corresponds to OHR_{ext} = 54 to 113 s^{-1} assuming k_OH_VOC = 5.33*10^{-11} cm^3 s^{-1}, and addition of 462 ppb isoprene corresponds to OHR_{ext} = 1136 s^{-1} assuming k_OH_VOC = 10^{-10} cm^3 s^{-1} (Atkinson et al., 1986). Results of our model runs are shown in the figure below:

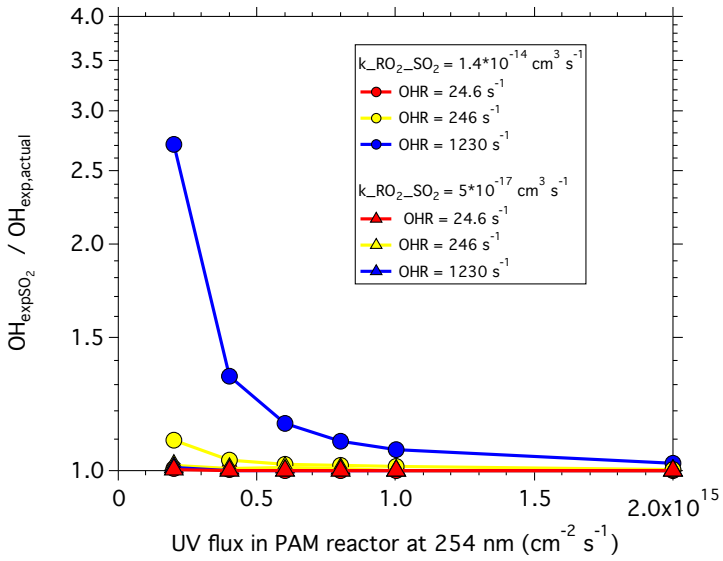

As is evident from the figure, application of the Kan et al. (1981) kinetic data (circles) suggests an overestimate of the OH exposure by up to factor of ~3 at Flux254 = 2*10^{14} cm^{-2} s^{-1} and OHR_{ext} = 1230 s^{-1}, which is equivalent to the addition of 500 ppbv isoprene to the PAM reactor. At higher UV intensity and/or lower OHR_{ext}, the overestimate in OH exposure is a factor of 1.3 or less. Application of the Sander and Walker (1981) kinetic data at the same operating conditions (triangles) reveals no effect of RO_2 + SO_2 reactions on the measured OH exposure.

Because of the aforementioned issues with the Kan et al. (1981) data, it is not clear that RO_2+SO_2 reactions affect our OH exposure calibrations.

References:

Sander, S. P. and R. T. Watson, A kinetic study of the reaction of SO_2 with CH_3O_2, *Chem. Phys. Lett.*, 77, 473-475, 1981.

Kurten, T., J. R. Lane, S. Jørgensen, and H. G. Kjaergaard, A Computational Study of the Oxidation of SO_2 to SO_3 by Gas-Phase Organic Oxidants, *J. Phys. Chem. A*, 115, 8669-8691, dx.doi.org/10.1021/jp203907d, 2011.

5) This concern about uncertainties in the quantitative OH exposure relates to Referee 2's comment about the authors' interpretation of Fig 5 that "It is not evident to me from Figure 5 that SOA yields at comparable OH exposures are a factor of 2 to 10 lower in the flow reactor than in chambers." For Fig 5a and Fig 5b, it appears that a decrease in OH exposure on order of a factor of ~2 would make the yields between the chamber and PAM indistinguishable for overlapping OH_{exp}. Therefore, unless the authors can demonstrate that the uncertainty in OH_{exp} is substantially less than a factor 2 with their methods, this statement should be removed from the paper (especially from the abstract and conclusions, where it appears in less quantitative terms), or possibly modified to reflect only the factor of 2-3 difference for isoprene SOA under the experimental conditions of these studies (and also probably the experimental agreement for the other compounds). Such low uncertainty of only a factor of 2 in OH_{exp} is difficult to achieve in practice with a PAM in our experience, and in any case requires careful work on this topic, something that cannot be assessed from the current version of the paper.

Response. Please see our response to Referee #2, Comment #5, where we revised the text as follows (changes in strikethrough):

P30587, L21-22: "1. SOA yields at comparable OH exposures are ~~a factor of 2 to 10~~ lower in the flow reactor than in chambers, whereas the mass spectra, O/C and H/C of SOA generated in the chambers and flow reactor are similar (Figs. 2–4)."

6) Meanwhile, only one chamber experiment from isoprene oxidation (in Fig 5a and Fig 6) was compared to the yield of isoprene in flow reactor experiments. However, isoprene SOA yields were also reported in other experiments, e.g., Kroll et al., (2006) found a yield range of 0.9%-3.6% for isoprene oxidation (low NO conditions) in chamber studies, which is lower than the chamber yield (~5.5%) used in this study and similar to the yield range in the PAM. A more comprehensive summary of published chamber yields should be included. Alternatively if there are reasons to exclude certain chamber studies, these should be given.

Response. For isoprene SOA, we are restricting the flow reactor/chamber comparison to data obtained without added NO_x and where the integrated OH exposure is provided (or can be calculated based on available information), as is stated on P30587, L10-11 of the discussions manuscript: "Figure 5 shows yields of SOA as a function of OH exposure for isoprene SOA (no added NO_x)." To our knowledge Kroll et al. (2006) is the only other chamber experiment (in addition to Chhabra et al., 2010) where these criteria are satisfied; thus, we have revised Figure

5a as shown below.

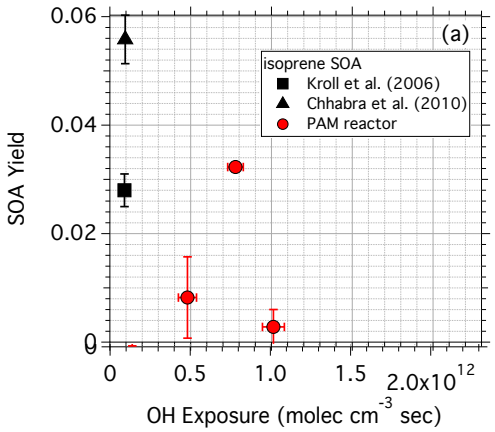

7) On a related point, what do the one-sigma uncertainties represent in Fig 5? Please clarify. As is, they may lead readers to assume they represent the uncertainty in the OH exposure (which is almost certainly much larger). They more likely represent ONLY the propagated variability from the measurements used to calculate it (rather than uncertainty in the offline/online calibration and/or models use to estimate OH_{exp}). An uncertainty analysis should be conducted to characterize the true uncertainties in OH_{exp}, which would help clarify whether the differences in yield in Fig 5 really have meaning.

Response. The Figure 5 caption states "Error bars indicate ±1σ uncertainty in binned measurements." The absolute uncertainty of OH exposures is presumably larger. Li et al. (2015) suggest an average ±34% uncertainty in OH exposure as measured using SO_2 tracer decay in an extensive series of OH exposure calibrations. We have revised Figure 5 and 6 (and captions) to incorporate this average ±34% OH exposure uncertainty as suggested by Li et al.

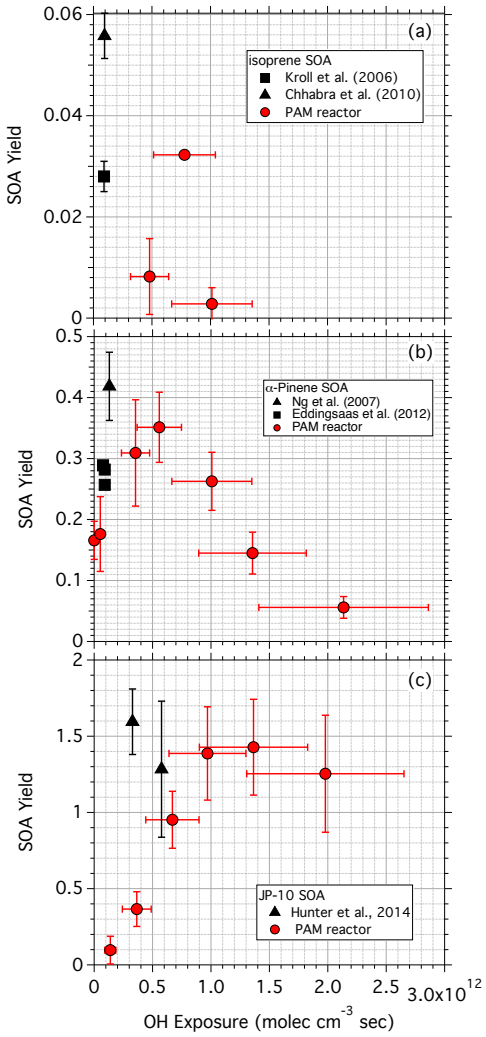

Figure 5. Yields of SOA produced from photoxidation of **(a)** isoprene, **(b)** α-pinene, and **(c)** tetracyclo[5.2.1.$0^{2,6}$]decane (JP-10) in environmental chambers and PAM reactor as a function of OH exposure. Error bars indicate ±1σ uncertainty in binned **SOA yield** measurements **and ±34% uncertainty in OH exposure values (Li et al., 2015)**. Black markers indicate data from **Kroll et al. (2006),** Chhabra et al. (2010), Eddingsaas et al. (2012), and Ng et al. (2007) obtained in the Caltech chamber and data from Hunter et al. (2014) ~~was~~ obtained in the MIT chamber.

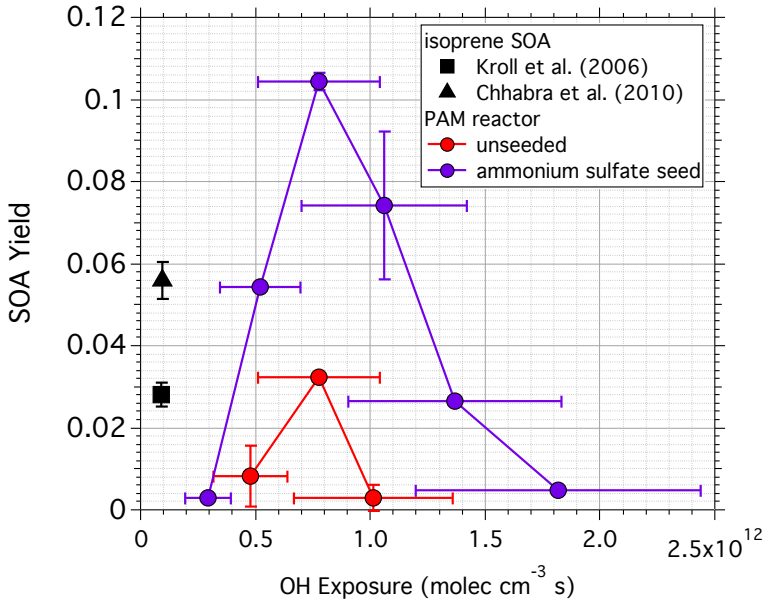

Figure 6. Yields of SOA produced from photoxidation of isoprene in the PAM reactor as a function of OH exposure in the presence of 20 μg m^{-3} ammonium sulfate seed. Error bars indicate ±1σ uncertainty in binned **SOA yield** measurements **and ±34% uncertainty in OH exposure values (Li et al., 2015).**

8) Table 1 and Figs 1-4 show that 8 different compounds were studied, however the yields are only discussed for 3 compounds. Why? Given that the yield results will likely be of the most interest to the community from this study, it would seem useful to discuss those results. This would give a better sense of the variability in the agreement/disagreement and provide better support for any generalizations and conclusions. As is, a reader quickly skimming the abstract and figures will assume that the yield conclusions broadly apply to the relatively wide range of compounds studied, which in current form is not supported in the manuscript.

Response. The yield conclusions apply to the rest of the compounds that were studied; thus, to simplify the presentation we focused on a representative subset that covered a range of different SOA yield values (isoprene SOA = low; α-pinene SOA = midrange; JP-10 SOA = high). We have revised the text to clarify this point (**changes bolded**):

P30587, L21-23: "SOA yields at comparable OH exposures are lower in the flow reactor than in chambers, whereas the mass spectra, O/C and H/C of SOA generated in the chambers and flow reactor are similar (Figs. 2–4). **Flow reactor SOA yields are also lower in the flow reactor than in chambers for the other precursors studied that are not shown in Figure 5.**"

9) OA concentrations have a major effect on SOA yields (as the authors point out as background in Sect. 3.4). However, the OA concentrations in the PAM vs chamber experiments in Fig 5 are not discussed in terms of their effect on the measured SOA yields. At least some of the chamber studies report OA-dependent yields, and the chamber yields should be corrected to the same OA concentrations observed in the flow reactor experiments.

Response. This is a fair point but in practice is difficult to identify overlap in OH exposure, precursor concentration reacted, and OA concentration. Our presentation in Figure 5 reflects the best overlap we could achieve. In our opinion even if it were possible to correct to the same OA concentration it would not alter the main conclusions of the figure and related discussion.

10) We suggest that Fig 7 should be plotted vs seed surface area, rather than mass, since condensation to seed aerosol or reactive uptake to an acidic seed aerosol would likely be a surface area-limited process.

Response. This is a good suggestion that we cannot readily implement for the sulfuric acid experiments. To obtain as many yield measurements as possible, the isoprene mixing ratio input to the PAM reactor was kept constant while varying the SO_2 mixing ratio in order to vary the sulfuric acid concentration. Characterization of the H_2SO_4 surface area at each condition would necessitate separate measurements of the sulfuric acid size distribution in the absence of isoprene SOA, which are not available. This would further require making the assumption that isoprene oxidation products do not interact with sulfuric acid vapor in the formation of new particles, which may not be the case.

11) Furthermore, it seems from the manuscript that the sulfuric acid (H_2SO_4) seed aerosol was produced by oxidation of SO_2 concurrent to isoprene oxidation in the flow reactor, in contrast to the atomized ammonium sulfate seed. Nucleation and atomization likely produced very different size distributions and thus very different surface area/mass ratios, potentially affecting the yields of SOA from isoprene. Also the size distribution in the nucleation experiments may lead to a significant fraction of SOA mass being too small to be measured by the AMS. The SMPS measurements from these experiments may help answer these questions.

Response. The SMPS mode volume-weighted diameter ranged from 122 to 217 nm in ammonium sulfate experiments and ranged from 195 to 241 nm in H_2SO_4 experiments. The AMS aerodynamic lens transmits particles with aerodynamic diameters ranging from about 60 to 600 nm with 100% efficiency, suggesting that most (if not all) of the mass is detected in the AMS. We added the following information to the text:

P30589-P30590, L26-4: "At an OH exposure of 7.8×10^{11} molec cm^{-3} s and a sulfate seed particle concentrations of 20 μg m^{-3}, the yield of isoprene SOA increases from 0.032 to approximately 0.14 in the presence of ammonium sulfate seeds and 0.25 in the presence of sulfuric acid seeds. **SMPS size distributions of the mixed particles suggest that most of the particle mass is measured by the AMS (Jayne et al., 2000).** Increasing the seed particle concentration led to a continued increase in the yield, along with a decrease in the O/C ratio of the SOA as condensation of less-oxidized products was enhanced."

The following citation was added to References:

J. T. Jayne, D. C. Leard, X. Zhang, P. Davidovits, K. A. Smith, C. E. Kolb, and D. R. Worsnop, Development of an Aerosol Mass Spectrometer for Size and Composition Analysis of Submicron Particles, Aerosol Science and Technology, 33, 49-70, 2000.

12) Comparison of the mass spectra in Fig 2 is very unclear. Larger log-log scatterplots, difference plots, or uncentered R^2 (Ulbrich et al., 2009) may be more useful. This topic was also alluded to by both referees.

Response. Please see our response to Comment #2 raised by Referee #2.

13) Particle wall losses in the reactor are quoted as 32% +/-15%. This is much higher than in our experience, where these losses are typically 5% in mass, when using an aluminum wall chamber. We observed losses of ~30% when using a glass cylindrical chamber as used in this study. As reported in Ortega et al., (2013), we believe the increased loss is due to nearly complete loss of charged particles to walls made of insulating material such as glass, Pyrex, or Teflon. In addition, very different charged-particle loss corrections need to be used when generating (charged) particles from an atomizer or (uncharged) particles by nucleation. Freshly atomized particles tend to be highly charged leading to even higher losses, and this effect can be reduced by passing the particles through a sufficiently potent radioactive neutralizer. It should be stated whether such neutralization was done or not in this study, so that it can help compare the likely particle losses in the experiments reported here with other studies. We suggest that the authors discuss these issues in some detail, as otherwise other groups may not be aware of the difference and apply the wrong loss correction in the future, thus significantly over or underestimating these effects.

Response. Atomized particles were not passed through a radioactive neutralizer. We revised the text to indicate this (changes bolded):

P30582, L9-L11: "The particles were dried and introduced continuously into the flow reactor along with the gas-phase SOA precursor **without radioactive charge neutralization."**

14) Page 30588, lines 4-12. The authors briefly discuss the time required for condensation, noting timescales of 2000-20,000 seconds, while the residence time in the reactor is 100 s. If those timescales represent e-fold timescales, that would suggest only 0.5-5% of the condensable products would condense in the reactor, rendering the PAM useless without large seed surface areas, which is clearly not the case. For example, if the isoprene yield was corrected by that condensation efficiency, SOA yields of ~60-600% would be implied. A more detailed discussion (including explicit calculation of the condensation timescales) is needed.

Response. We modified the text as follows (changes bolded).

"One reason for the lower SOA yield in flow reactors may be the relative timescales for oxidation in the gas-phase vs. condensation onto pre-existing aerosols. **The timescale for condensation of a gas-phase molecule onto pre-existing seed particles (τ_{cond}) can be calculated using Equation 1 (Seinfeld and Pandis, 2006):**

$$\tau_{cond} = \frac{1}{\alpha * A_p} \sqrt{\frac{2\pi M_w}{k_B T}} \quad [1]$$

Where M_w is the molecular weight of the condensing species, α is the mass accommodation coefficient, and A_p is the particle surface area. For example, over a representative range of particle surface area concentrations used in the flow reactor (10 to 100 μm^2 cm^{-3}), condensation timescales range from approximately 2000 to 20000 s assuming a mass accommodation coefficient of 0.1 (**α-pinene ozonolysis SOA;** Saleh et al., 2013) and an average SOA molecular weight of 150 g mol^{-1}. **A lower limit of τ_{cond} = 200 to 2000 s is calculated over the same range of A_p assuming α = 1.** While our measurements do not constrain the mass accommodation coefficient, these timescales suggest that the residence time in the flow reactor (100 s) may not be adequate to allow complete condensation of semivolatile organic gas-phase species into SOA**, whereas residence times in environmental chamber experiments are typically 10000 sec or longer**."

We would like to reiterate that we did not constrain the mass accommodation coefficient in our measurements. As noted in the revised text, the α = 0.1 result reported by Saleh et al. (2013) corresponds to α-pinene ozonolysis SOA; no literature values of accommodation coefficients for isoprene SOA are available, so this accommodation coefficient may or may not be representative of isoprene oxidation products.

The following citation has been added to references:

Seinfeld J. H. and Pandis S. N., Atmospheric Chemistry and Physics: From Air Pollution to Climate Change, 2nd edition, J. Wiley, New York, 2006.

15) Seed experiments were shown only for isoprene, which is the only compound with evidence for lower yields in PAM compared to a chamber experiment. However, the authors conclude at the end of Sect. 3.5 "these measurements suggest seed particles are required in flow reactor measurements in order to more closely simulate condensation conditions in environmental chambers." Such a general statement is not supported and should be modified accordingly.

Response. We revised the text as follows (changes bolded):

P30590, L10-12: "These measurements suggest seed particles are required in flow reactor measurements **of isoprene SOA (and potentially other types of SOA as well)** in order to more closely simulate condensation conditions in environmental chambers."

[1,2]A. T.Lambe [2,*]P. S.Chhabra [1,2]T. B.Onasch [3]W. H.Brune [4]J. F.Hunter [4]J. H.Kroll [1]M. J.Cummings [1]J. F.Brogan [1]Y.Parmar [2]D. R.Worsnop [2]C. E.Kolb [1]P.Davidovits
Manuscript prepared for J. Name
with version 5.0 of the LaTeX class copernicus.cls.
Date: 13 February 2015

~~Comparison of secondary organic aerosol formed with an aerosol flow reactor and environmental reaction chambers:~~ Effect of oxidant concentration, exposure time and seed particles on secondary organic aerosol chemical composition and yield

Chemistry Department, Boston College, Chestnut Hill, MA, USA

Aerodyne Research Inc., Billerica, MA, USA

Department of Meteorology and Atmospheric Sciences, The Pennsylvania State University, State College, PA, USA

Department of Civil and Environmental Engineering, Massachusetts Institute of Technology, Cambridge, MA, USA

now at: Department of Chemical Engineering, University of Texas, Austin, Texas, USA

Correspondence to: A. T. Lambe (lambe@aerodyne.com)

Abstract. We performed a systematic intercomparison study of the chemistry and yields of SOA generated from OH oxidation of a common set of gas-phase precursors in a Potential Aerosol Mass (PAM) continuous flow reactor and several environmental chambers. In the flow reactor, SOA precursors were oxidized using OH concentrations ranging from 2.0×10^8 to 2.2×10^{10} molec cm^{-3} over exposure times of 100 s. In the environmental chambers, precursors were oxidized using OH concentrations ranging from 2×10^6 to 2×10^7 molec cm^{-3} over exposure times of several hours. The OH concentration in the chamber experiments is close to that found in the atmosphere, but the integrated OH exposure in the flow reactor can simulate atmospheric exposure times of multiple days compared to chamber exposure times of only a day or so. In most cases, for a specific SOA type the most-oxidized chamber SOA and the least-oxidized flow reactor SOA have similar mass spectra, oxygen-to-carbon and hydrogen-to-carbon ratios, and carbon oxidation states at integrated OH exposures between approximately 1×10^{11} and 2×10^{11} molec cm^{-3} s, or about 1-2 days of equivalent atmospheric oxidation. This observation suggests that in the range of available OH exposure overlap for the flow reactor and chambers, SOA elemental composition as measured by an aerosol mass spectrometer is similar whether the precursor is exposed to low OH concentrations over long exposure times or high OH concentrations over short exposure times. ~~A linear correlation analysis of the mass spectra ($m = 0.91$–0.92, $r^2 = 0.93$–0.94) and carbon oxidation state ($m = 1.1$, $r^2 = 0.58$) of~~

~~SOA produced in the flow reactor and environmental chambers for OH exposures of approximately 10^{11} molec cm^{-3} s suggests that the composition of SOA produced in the flow reactor and chambers is the same within experimental accuracy as measured with an aerosol mass spectrometer.~~ This similarity in turn suggests that both in the flow reactor and in chambers, SOA chemical composition at low OH exposure is governed primarily by gas-phase OH oxidation of the precursors, rather than heterogeneous oxidation of the condensed particles. In general, SOA yields measured in the flow reactor are lower than measured in chambers for the range of equivalent OH exposures that can be measured in both the flow reactor and chambers. The influence of sulfate seed particles on isoprene SOA yield measurements was examined in the flow reactor. The studies show that seed particles increase the yield of SOA produced in flow reactors by a factor of 3 to 5 and may also account in part for higher SOA yields obtained in the chambers, where seed particles are routinely used.

1 Introduction

Laboratory and field studies over the last decade have shown that organic components of atmospheric particles constitute 20 to 50 % of the fine particle mass (PM) in the continental mid-latitudes, though the organic content can be higher (up to 90 %) in tropical forested regions (Kanakidou et al., 2005). On a global scale, 50–90 % of submicron organic PM is composed of oxygenated organic aerosol (Zhang et al., 2005) that is typically associated with secondary organic aerosol (SOA) formed by condensation of oxidized gas-phase species (Jimenez et al., 2009). Field studies indicate that SOA particles may influence cloud formation (Levin et al., 2014; Mei et al., 2013; Moore et al., 2012; Sihto et al., 2011) and may be optically active in the UV/Visible region of the electromagnetic spectrum (Zhang et al., 2011). These studies have also revealed the complexity of organic aerosol compositions and their chemical evolution via oxidative aging. The atmospheric lifetime of ambient SOA ranges from hours to weeks, providing a wide range of atmospheric exposures to a variety of oxidant species. Measured ambient SOA chemical compositions range from hydrocarbon-like organic aerosol, such as observed directly downwind of the Deepwater Horizon oil site during the 2010 Gulf Oil Spill (Bahreini et al., 2012; De Gouw et al., 2011), to highly oxygenated OA, such as background SOA observed worldwide (Zhang et al., 2007). Much of this complexity is due to the thousands of organic compounds found in atmospheric particulate matter, specifically low volatility, highly functionalized species (Hallquist et al., 2009).

Laboratory experiments conducted in environmental chambers have been essential in providing SOA physical and chemical properties as well as yield data for predicting the rate of atmospheric SOA formation due to oxidation of biogenic and anthropogenic volatile organic compounds (VOCs) (Spracklen et al., 2011). Substantial progress has been made in understanding reaction mechanisms and the factors that influence SOA yields and composition. For example, SOA yields appear to have a complex dependence on VOC : NO_x ratio (Loza et al., 2014; Ng et al., 2007), precursor concen-

tration/volatility (Presto and Donahue, 2006), and oxidant exposure (Lambe et al., 2012). Modeling observed atmospheric SOA levels therefore remains a challenge (Shrivastava et al., 2011; Bergström et al., 2012; Jo et al., 2013; Li et al., 2013) because of the large number of modeling parameters and associated sensitivities that are required to capture mechanistic details of SOA formation (Chen et al., 2013; Fountoukis et al., 2014).

Oxidant exposure is the integral of the oxidant species concentration and the sample residence time. Relatively low oxidant exposures are a major limitation of current environmental chamber techniques, which operate at OH concentrations ranging from approximately 10^6 to 10^7 molec cm^{-3} that are equal to or slightly more than daytime atmospheric OH concentrations. Chamber experiments are generally limited to residence times of several hours due to chamber deflation and the loss of oxidized vapors (Zhang et al., 2014) and/or particles to the chamber walls. This combination of low OH concentrations and residence time limits environmental chambers to simulating atmospheric aerosol particle lifetimes only up to 1 or 2 days, including the characterization of SOA yields. This limitation prevents the formation and the study of highly oxygenated SOA that is characteristic of aged atmospheric organic aerosol PM (Ng et al., 2010).

Recently, aerosol flow reactors have been developed to study SOA formation and evolution equivalent to multiple days of atmospheric OH exposure. In these reactors OH concentrations are typically $\sim 10^9$ molec cm^{-3} or greater, with reactor residence times of seconds to minutes (Kang et al., 2007; Hall IV et al., 2013; Keller and Burtscher, 2012; Lambe et al., 2011a; Slowik et al., 2012). With this range of OH concentrations and exposure times, flow reactors can simulate the full range of ambient levels of oxidation, measuring changes in SOA composition and yields over a wide range of equivalent atmospheric oxidation. Further, because of the short flow reactor residence times, experimental runs can be conducted on the scale of minutes rather than hours.

While flow reactors appropriately simulate the full range of integrated atmospheric oxidant exposures, in view of their short residence times and high oxidant concentrations it must be established how well the atmospheric aerosol chemistry is simulated (Renbaum and Smith, 2011). A growing set of studies indicates that flow reactor-generated SOA particles have compositions similar to ambient SOA, suggesting that the dominant oxidation reaction pathways in flow reactors are similar to those in ambient conditions (Bahreini et al., 2012; Lambe et al., 2012, 2011b; Kang et al., 2011; Massoli et al., 2010; Ortega et al., 2013; Slowik et al., 2012; Wang et al., 2012; Wong et al., 2011). Other studies have used a combination of aerosol flow reactors and environmental chambers to characterize heterogeneous uptake of organics on seed particles (Jang et. al., 2003), SOA formation potential (Kang et al., 2007; Bernard et al., 2012), and evolution of functional groups in SOA with aging (Ofner et al., 2010); in general, similar results are obtained in reactors and chambers. However, these comparisons need to be extended over a wider range of reactants and experimental conditions than are currently available.

Here we describe systematic intercomparison studies of SOA chemistry and yields generated from

a common set of precursors in a Potential Aerosol Mass (PAM) flow reactor (Lambe et al., 2011a) and four environmental chambers. SOA precursors studied are gas-phase alkane, biogenic, and aromatic compounds. SOA chemical composition and yield were characterized as a function of OH exposure. Additionally, the effect of sulfate seed particles on isoprene SOA yields was studied. Due to the limited oxidative exposure provided by the environmental chambers, direct comparison between the two techniques is possible only over a narrow range. However, reasonable extrapolations extend the range of interest.

2 Experimental

This manuscript compares properties of SOA produced in the PAM reactor to SOA produced in environmental chambers operated at the four institutions: California Institute of Technology (Caltech), Massachusetts Institute of Technology (MIT), Paul Scherrer Institut (PSI), and Carnegie Mellon University (CMU). The PAM reactor is a horizontal 13.3 L glass cylindrical chamber, $46\,\mathrm{cm\,long}\times22\,\mathrm{cm}$ ID and is operated in continuous flow mode with an average residence time of 100 s. The RH in the reactor was controlled in the range of 30–40 %. The Caltech, MIT, PSI and CMU Teflon chambers range from 7.5 to 28 m^3 in volume and are operated in batch or semi-batch mode with experimental residence times ranging from 4 to 10 h. The relative humidity (RH) in the Caltech, MIT and CMU chamber experiments was less than 10 %, and the RH in the PSI chamber experiments was controlled in the range of 40–50 %. A summary of the methods used for OH radical generation, particle generation, and data analysis is provided below.

2.1 OH radical generation

In the flow reactor, OH radicals were produced in the absence of $\mathrm{NO_x}$ via the reaction $\mathrm{O(^1D) + H_2O \rightarrow 2OH}$, with $\mathrm{O(^1D)}$ radicals produced from the reaction $\mathrm{O_3} + h\nu \rightarrow \mathrm{O_2} + \mathrm{O(^1D)}$. $\mathrm{O_3}$ (15 - 30 ppm) was generated by $\mathrm{O_2}$ irradiation with a mercury lamp ($\lambda = 185\,\mathrm{nm}$) outside the flow reactor. The $\mathrm{O(^1D)}$ atoms were produced by UV photolysis of $\mathrm{O_3}$ inside the flow reactor using four mercury lamps which emit primarily at λ = 254 nm. Additional photons are emitted at the following wavelengths with relative intensities of 1% or more of the UV intensity at 254 nm: 185 nm (1% Li et. al. (2015)); 302 nm (1%); 313 nm (1%); 366 nm (1%); 405 nm (1%); 436 nm (10%); 546 nm (1%) (BHK Inc. product specifications). At the highest UV intensity that was used in the reactor, we calculate upper-bound J_{UV} = 2×10^{13} and 2×10^{15} $\mathrm{cm^{-2}}s^{-1}$ at λ = 185 and 254 nm from ozone and OH exposure measurements. Corresponding lower limit timescales for UV photolysis of several phenols, carboxylic acids, aldehydes and ketones range from 12 to 50,000 sec for absorption cross sections ranging from approximately 4×10^{-17} to 1×10^{-20} $\mathrm{cm^3\ molec^{-1}\ s^{-1}}$ (https://sites.google.com/site/pamwiki/ and references therein).

In offline calibrations, OH concentrations were varied by changing the UV light intensity through

stepping the lamp voltages between 0 and 110V. SO_2 was added to the carrier gas, typically at mixing ratios ranging from 30 to 60 ppbv, and was used as an OH tracer. Calibrations were conducted at the same H_2O and O_3 concentrations used in SOA experiments. At each lamp setting, OH exposures were quantified by measuring the steady-state SO_2 mixing ratio and normalizing to the SO_2 mixing ratio obtained with the lamps turned off. The corresponding OH exposure was quantified by ~~measuring the decay of SO_2~~ normalizing the SO_2 mixing ratio with the lamps on to the SO_2 mixing ratio with the lamps off and applying the known $OH + SO_2$ rate constant (Davis et al., 1979), as shown in Equation 1:

$$\mathrm{OH\,exposure} = -\frac{1}{k_{SO_2}^{OH}} \ln\left(\frac{[SO_2]}{[SO_2]_i}\right) \quad (1)$$

The concentrations ranged from approximately 2.0×10^8 to 2.2×10^{10} molec cm^{-3}. The corresponding OH exposures ranged from 2.0×10^{10} to 2.2×10^{12} molec cm^{-3} s or approximately 0.2 to 17 days of equivalent atmospheric exposure. Additional SO_2 calibration measurements were conducted in the presence and absence of a subset of precursors (isoprene and JP-10) to investigate reductions in OH levels following addition of those precursors to the flow reactor at mixing ratios that were used in SOA experiments. No change in SO_2 decay was observed upon addition of isoprene, but addition of JP-10 decreased OH levels by approximately 10% (highest OH exposure) to 50% (lowest OH exposure) (Lambe et al., 2012). Reductions in OH exposure following addition of other VOCs will be investigated in future work using the methods of Li et. al. (2015).

In the environmental chambers, OH radicals were generated by UV photolysis ($\lambda = 350$ nm) of hydrogen peroxide (H_2O_2) with no added NO_x, or by UV photolysis of nitrous acid (HONO) or methyl nitrite (CH_3ONO) with NO_x. In the present studies, OH radicals generated in the Caltech chamber were formed from photolysis of H_2O_2, HONO, or CH_3ONO, depending on the experiment, whereas OH radicals generated in the MIT, PSI and CMU chambers were formed exclusively from HONO photolysis. Typical chamber OH concentrations were approximately 2×10^6 molec cm^{-3} (H_2O_2) and 2×10^7 molec cm^{-3} (HONO) during the initial stage of chamber experiments. Corresponding OH exposures ranged from 5.4×10^{10} to 4.0×10^{11} molec cm^{-3} s (Tab. 1), equivalent to approximately 0.4 to 3 days of atmospheric exposure at a typical 24 h average OH concentration of 1.5×10^6 molec cm^{-3} (Mao et al., 2009).

2.2 Particle generation

~~Figure ?? shows~~ The gas-phase SOA precursors used in these studies include two biogenic compounds ~~gases~~ (isoprene, α-pinene), three aromatic compounds (toluene, m-xylene, naphthalene), and three alkanes (n-C_{10}, cyclodecane, tricyclo[5.2.1.0^{2,6}]decane, also known as JP10). In the flow reactor, SOA was generated via gas-phase OH oxidation of precursors followed by homogeneous nucleation, or by condensation onto sulfuric acid or ammonium sulfate seed particles. The sulfuric

acid seed particles were generated by OH oxidation of SO_2 together with the SOA precursor, and ammonium sulfate seed particles were generated by atomizing an ammonium sulfate solution. The particles were dried and introduced continuously into the flow reactor (without radioactive charge neutralization) along with the gas-phase SOA precursor. In environmental chambers, SOA was generated via gas-phase OH oxidation of precursors usually followed by condensation onto ammonium sulfate seed particles. For long residence time chamber experiments, wall condensation of precursor gas-phase species can be significant. Seed particles are used in chamber studies to reduce wall effects. In some of the flow reactor experiments seed particles were also used to study their effect on SOA yields.

2.3 Particle monitoring and analysis

Particle number concentrations and size distributions were measured with a TSI scanning mobility particle sizer (SMPS). Aerosol mass spectra were measured with an Aerodyne time-of-flight aerosol mass spectrometers (ToF-AMS) (DeCarlo et al., 2006; Drewnick et al., 2005). Elemental analysis (Aiken et al., 2008) was performed on the AMS data to determine the bulk aerosol hydrogen-to-carbon (H/C) and oxygen-to-carbon (O/C) ratios along with the average aerosol carbon oxidation state ($\overline{OSc}$) (Kroll et al., 2011). While AMS measurements provide basic information about SOA composition, additional supporting measurements such as Fourier transform infrared spectroscopy, nuclear magnetic resonance, gas chromatography ass spectrometry, and chemical ionization mass spectrometry are required to investigate SOA chemistry at the molecular level.

SOA yields were calculated from the ratio of aerosol mass formed to precursor gas reacted. The aerosol mass was calculated from the integrated particle volume and the effective particle density ($\rho = D_{va}/D_m$), where D_{va} is the mean vacuum aerodynamic diameter obtained from the ToF-AMS and D_m is the electric mobility diameter obtained from the SMPS. Flow reactor SOA yields were corrected using size-dependent bis(2-ethylhexyl) sebacate wall-loss measurements (Lambe et al., 2011a); the average magnitude of these corrections was 32 % (±15 %) and represents an upper limit as it combines losses into and through the reactor. Caltech chamber yields were corrected for particle wall losses using size-dependent first-order loss coefficients determined from ammonium sulfate wall-loss measurements (Keywood et al., 2004). The magnitude of these particle wall loss corrections typically ranged from 10–30 %.

MIT chamber experiments were corrected for particle wall losses using the AMS organic-to-sulfate ratio to generate an upper limit and SMPS measurements of particle loss to generate a lower limit for aerosol yield (Hildebrandt et al., 2009). In the MIT chamber, these corrections were between a factor of 1.5 to 3.0 at the highest yields and OH exposures. Although the residence time in the flow reactor is much shorter than in the chambers, the surface-to-volume ratio in the PAM reactor is much greater. As a result particle losses are comparable in the two systems. Flow reactor SOA yields were also corrected for UV lamp-induced temperature increases by applying yield cor-

rections of -0.02 per ~~degree~~ K of temperature rise (Qi et al., 2010; Stanier et al., 2007) relative to room temperature (~ 293 K). These temperature corrections ranged from 0–28 % (mean correction $\pm 1\sigma = 7 \pm 7$ %). In the flow reactor, a known amount of precursor gas was introduced and the mass of reacted precursor gas was estimated from the OH exposure and known bimolecular rate constants (Atkinson, 1986). In environmental chamber studies, the mass of the remaining precursor gas was measured directly as a function of exposure time.

3 Results and discussion

3.1 Sample mass spectra of flow reactor- and chamber-generated SOA

Figure 1 shows representative ToF-AMS spectra of SOA generated in the PAM reactor and the Caltech chamber (Chhabra et al., 2010, 2011) from the OH oxidation of α-pinene and naphthalene, used here as representative biogenic and anthropogenic precursors respectively. The flow reactor spectra are obtained at an OH exposure of 1.6×10^{11} molec cm^{-3} s, or ~ 1 day of equivalent atmospheric oxidation. The chamber spectra represent the SOA composition at peak aerosol formation ($\sim 9 \times 10^{10}$ molec cm^{-3} s OH exposure). In this range the OH exposure for the PAM reactor and chamber are approximately the same, allowing for direct comparison. To quantify the similarity between mass spectra, we calculated the dot product between SOA mass spectra generated in the PAM flow reactor and the Caltech chamber (Murphy et. al., 2003; Marcolli et al., 2006). Using this approach, each mass spectral signal is normalized to the square root of the sum of the squares of all signals in the mass spectrum. Each spectrum is represented as a normalized vector A or B, with dot product A· B = $\Sigma_{i=1}^{n} a_i b_i$, where a_i and b_i are the normalized signals at each *m/z* in the spectrum; A · B = 0 indicates the spectra are orthogonal and A· B = 1 indicates the spectra are identical.

The top table inset in Fig. 1 shows the calculated dot products between each pair of mass spectra. The PAM flow reactor and the chamber produce particles with similar mass spectra, as indicated by dot products of 0.97 between spectra shown in Figs. 1a and c (α-pinene SOA) and Figs. 1b and d (naphthalene SOA), suggesting similar compositions. ~~The PAM flow reactor and the chamber produce particles with similar mass spectra, suggesting similar compositions~~. Features unique to α-pinene and naphthalene SOA are observed in both flow reactor- and chamber-obtained spectra, with linear correlation coefficients of $r^2 = 0.93$ (α-pinene SOA) and $r^2 = 0.94$ (naphthalene SOA) as noted in the bottom table inset in Fig. 1. For example, α-pinene SOA spectra are dominated by signals at $m/z = 43$ ($C_2H_3O^+$) indicative of carbonyls, and several ion clusters below $m/z < 100$ containing signals that are indicative of cycloalkyl fragments such as $m/z = 27$, 41, and 55. On the other hand, AMS spectra of naphthalene SOA are dominated by $m/z = 44$ (CO_2^+), indicative of carboxylic acids, as well as signals that are indicative of aromatic compounds such as $m/z = 50$–51, 65, and 76–77. As is evident from Fig. 1, α-pinene and naphthalene SOA mass spectra display pronounced differences, with dot products ranging from 0.42 to 0.63 and r^2 ranging from 0.18 to

0.37 between spectra shown in Figs. 1a and b, 1a and d, 1b and c, and 1c and d.

3.2 H/C, O/C ratios for flow reactor- and chamber-generated SOA

H/C and O/C ratios obtained from mass spectra such as shown in Fig. 2 provide information about the nature of SOA formation. Van Krevelen diagrams that show H/C ratios as a function of O/C ratios have been used to deduce oxidation reaction mechanisms for organic aerosols (Heald et al., 2010). Typically, with oxidative aging the O/C ratio increases and H/C ratio of SOA decreases as oxygen-containing functional groups are added to a carbon backbone. Here, we use Van Krevelen diagrams to compare the composition of SOA formed in the flow reactor and environmental chambers for the organic precursors studied. Direct comparisons are possible in the overlapping OH exposure region. Typically the lowest OH exposures attained in the flow reactor overlap (or nearly overlap) with the highest OH exposures reached in environmental chambers (Table 1).

Figure 2 shows Van Krevelen diagrams obtained from laboratory SOA produced from the oxidation of gas-phase biogenic, aromatic, and alkane precursors. To simplify presentation, the data are displayed in three panels. Figure 2a shows biogenic SOA generated from isoprene and α-pinene, Fig. 2b shows SOA generated from aromatic compounds, and Fig. 2c shows SOA produced from alkanes. In most cases, for a specific SOA type the most-oxidized chamber SOA and the least-oxidized flow reactor SOA have similar Van Krevelen plots at integrated OH exposures between approximately 1×10^{11} and 2×10^{11} molec cm^{-3} s, or about 1–2 days of equivalent atmospheric oxidation. This observation suggests that in the range of available OH exposure overlap for the flow reactor and chambers, SOA elemental composition is similar whether the precursor is exposed to low OH concentrations over long exposure times or high OH concentrations over short exposures times. The flow reactor studies were done without added NO_x, whereas some of the environmental chamber studies were conducted in the presence of NO_x. The similarity in compositional parameters shown in Fig. 2 (e.g. H/C, O/C) were independent of the NO_x levels used in the environmental chambers in the region studied, as has been observed in previous studies (Chhabra et al., 2011). The nitrogen-to-carbon (N/C) ratio ranged from 0.031 to 0.054 for SOA produced in the MIT chamber with added NO_x (Hunter et al., 2014) but was not characterized for other measurements shown in Fig. 2.

3.3 Carbon oxidation state for flow reactor- and chamber-generated SOA

Recently, the average carbon oxidation state ($\overline{OSc}$), defined as $\overline{OSc} = 2 \times O/C - H/C$, was proposed as a more accurate indicator of atmospheric oxidative aging processes than the O/C ratio alone because this measure takes into account the level of saturation of the carbon atoms in the SOA (Canagaratna et al., 2014; Kroll et al., 2011). As will be demonstrated, $\overline{OSc}$ of lightly oxidized SOA is strongly precursor-dependent. Figure 3 shows a scatter plot of $\overline{OSc}$ for flow reactor and chamber SOA for the eight gas-phase precursors studied. Different colored symbols are used to represent

each of the environmental chambers used in the intercomparison. For each data point obtained from environmental chamber measurements, we used data from the flow reactor obtained at the OH exposure that was closest in magnitude. A total linear least squares fit to the data presented in Fig. 3 ($\mathrm{PAM}_{\overline{\mathrm{OSc}}} = 1.1 \cdot \mathrm{Chamber}_{\overline{\mathrm{OSc}}} - 0.16$; $r^2 = 0.54$) indicates that there is no systematic $\overline{\mathrm{OSc}}$ difference observed across multiple SOA types produced in chambers and in flow reactors. For a specific SOA type, Figure 3 shows that the chambers and flow reactor provide ~~similar~~ $\overline{\mathrm{OSc}}$ ~~for a specific SOA type~~ with absolute differences ranging from 0.0040 to 0.60 (mean deviation = 0.10 $\pm$ 0.34) over the range of measured SOA composition for comparable OH exposures. The observed deviations between PAM and chamber $\overline{\mathrm{OSc}}$ are no larger than deviations between two chambers (e.g. α-pinene SOA produced in Caltech and PSI chambers, and cyclodecane SOA produced in MIT and CMU chambers).

3.4 SOA yields obtained in the flow reactor and environmental chambers

Several factors can affect SOA yields, including precursor concentration (Kang et al., 2011; Pfaffenberger et al., 2013; Presto and Donahue, 2006), $\mathrm{NO_x}$ (Presto et al., 2005; Ng et al., 2007), UV intensity/wavelength (Henry and Donahue, 2012), seed particle composition/loading (Ehn et al., 2014; Hamilton et al., 2011; Volkamer et al., 2009) and treatment of interactions between SOA and chamber walls (Hildebrandt et al., 2009; Matsunaga and Ziemann, 2010; Pierce et al., 2008; Zhang et al., 2014). For reference, the range of SOA precursor concentrations, $\mathrm{NO_x}$ levels, and seed particle concentrations used in SOA yield studies is summarized in Table 2. Isolation of individual factors is beyond the scope of this intercomparison. Because mass spectra and elemental ratios of SOA are similar whether it is generated in an environmental chamber or in a flow reactor (Sec. 3.1), we suggest that the differences in precursor concentration and UV wavelength (e.g. $\lambda = 350\,\mathrm{nm}$ vs. $\lambda = 254\,\mathrm{nm}$) used in these studies have at most a minor effect on bulk composition.

Next we evaluate the influence of oxidant concentration and residence time on yields of SOA formed from common precursors in the PAM reactor and the Caltech and MIT environmental chambers. Figure 4 shows yields of SOA as a function of OH exposure for isoprene SOA (no added $\mathrm{NO_x}$), α-pinene SOA (no added $\mathrm{NO_x}$), and tricyclo[5.2.1.$0^{2,6}$]decane (JP-10) SOA, respectively. These precursors provide the broadest range of available yield values for intercomparison. Oxidation of isoprene forms SOA with low yield (Chhabra et al., 2010; Kroll et al., 2006), whereas α-pinene forms SOA with moderate yields (Eddingsaas et al., 2012) and JP-10 forms SOA with mass yields greater than unity (Hunter et al., 2014; Lambe et al., 2012). Yields of alkane SOA do not display a systematic $\mathrm{NO_x}$ dependence (Loza et al., 2014); thus, to first order we assume different $\mathrm{NO_x}$ levels between the MIT chamber and PAM reactor do not influence our comparison of measured JP-10 SOA yields. The following features are evident in Fig. 4:

1. SOA yields at comparable OH exposures are ~~a factor of 2 to 10~~ lower in the flow reactor than in chambers, whereas the mass spectra, $\mathrm{O/C}$ and $\mathrm{H/C}$ of SOA generated in the chambers and

flow reactor are similar (Figs. 1–3). Flow reactor SOA yields are also lower in the flow reactor than in chambers for the other precursors studied that are not shown in Fig. 4.

2. SOA yields in the flow reactor and chambers track each other; that is, the maximum yield of isoprene SOA is approximately 0.03 in the flow reactor and 0.06 in the Caltech chamber (Fig. 4a). Likewise, the maximum yield of JP-10 SOA is 1.4 in the flow reactor and 1.6 in the MIT chamber (Fig. 4c).

3. In the flow reactor, in all cases the SOA yield first increases as a function of OH exposure and then decreases. In some cases there is also evidence of a slight decrease in SOA yields at higher OH exposure in chambers (e.g. Fig. 4c).

One reason for the lower SOA yield in flow reactors may be the relative timescales for oxidation in the gas-phase vs. condensation onto pre-existing aerosols. The timescale for condensation of a gas-phase molecule onto pre-existing seed particles (τ_{cond}) can be calculated using Eq. 2 (Seinfeld and Pandis, 2006):

$$\tau_{\mathrm{cond}} = \frac{1}{\alpha \mathrm{A_p}} \sqrt{\frac{2\pi \mathrm{M_w}}{\mathrm{k_B T}}} \tag{2}$$

Where M_w is the molecular weight of the condensing species, α is the mass accommodation coefficient, and A_p is the particle surface area. For example, over a representative range of particle surface area concentrations used in the flow reactor (10 to 100 $\mu m^2\,cm^{-3}$), condensation timescales range from approximately 2000 to 20 000 s assuming a mass accommodation coefficient of 0.1 as has been measured for α-pinene ozonolysis SOA (Saleh et al., 2013) and an average SOA molecular weight of 150 $g\,mol^{-1}$. A lower limit of τ_{cond} = 200 to 2000 s is calculated over the same range of A_p assuming α = 1. While our measurements do not constrain the mass accommodation coefficient, these timescales suggest that the residence time in the flow reactor (100 s) may not be adequate to allow complete condensation of semivolatile organic gas-phase species into SOA, whereas residence times in environmental chamber experiments are typically 10000 s or longer. Another factor in causing the SOA yield difference may be due to the condensation conditions. All the chamber experiments displayed in this work were done in the presence of ammonium sulfate seed particles, whereas seed particles were not normally used in our flow reactor studies. The effect of seed particles on SOA yields in the flow reactor is examined further in Sect. 3.5.

The observation that the yields track each other is a further indication that the reactive chemistry in the two systems is similar. The decrease in SOA yield subsequent to increase as a function of OH exposure is possibly due to gas-phase species carbon-carbon bond breaking from continued oxidation or heterogeneous OH oxidation reactions at high OH exposure (Hunter et al., 2014; Lambe et al., 2012; Loza et al., 2012); this trend is most clearly evident in the flow reactor studies. These

observations suggest that the first step in SOA formation is oxidation of gas-phase species leading to subsequent condensation. At low OH exposures equivalent to 1–2 days, heterogeneous reactions do not appear to play a significant role in SOA chemistry (Cappa and Wilson, 2012; Chen et al., 2013).

3.5 Effect of seed particles on SOA yields

The chamber experiments discussed in Sects. 3.1–3.4 were performed in the presence of ammonium sulfate seeds to promote more rapid condensation of gas-phase species into SOA. We investigated in more detail the influence of sulfate seed particle loading and composition on SOA yields produced in the flow reactor. We hypothesize that a "seed effect" should be most pronounced for SOA types with low yields, and investigate this proposal for isoprene SOA whereas the effect of sulfate seeds on α-pinene SOA yields is minor (Kang et al., 2007). Figure 5 shows isoprene SOA yields in the flow reactor as a function of OH exposure using an ammonium sulfate seed particle mass concentration of $20\,\mu g\,m^{-3}$ which is comparable to sulfate volume concentrations used by Chhabra et al. (2010). At an OH exposure of $2.9 \times 10^{11}\,molec\,cm^{-3}\,s$ or less in the flow reactor, the isoprene SOA yield with seeds added to the flow reactor compared to the SOA yield in the Caltech chamber is negligible. As the OH exposure is increased in the flow reactor, the SOA yield rises to a maximum value of 0.10 at $7.8 \times 10^{11}\,molec\,cm^{-3}\,s$ OH exposure and then decreases. We note that the same trend was observed without adding seed particles, although with lower SOA yields. The O/C ratio of the flow reactor SOA decreases from 0.63 to 0.59 when seeds are added at $7.8 \times 10^{11}\,molec\,cm^{-3}\,s$ OH exposure. Figure 5 supports the hypothesis that addition of seed particles promotes condensation, leading to higher SOA yields. Higher concentrations of seed particles may be required for condensation of gas-phase oxidation products to compete with continued OH oxidation in the gas phase.

To further investigate the effect of seeds on condensation, we measured isoprene SOA yields as a function of ammonium sulfate and sulfuric acid seed particle concentrations (Fig. 6). An OH exposure of $7.8 \times 10^{11}\,molec\,cm^{-3}\,s$ was used in the flow reactor because this condition provided the best signal-to-noise ratio. It is evident from these figures that adding sulfate seeds significantly increases the SOA yield. At an OH exposure of $7.8 \times 10^{11}\,molec\,cm^{-3}\,s$ and a sulfate seed particle concentrations of $20\,\mu gm^{-3}$, the yield of isoprene SOA increases from 0.032 to approximately 0.14 in the presence of ammonium sulfate seeds and 0.25 in the presence of sulfuric acid seeds. SMPS size distributions of the mixed particles suggest that most of the particle mass is measured by the AMS (Jayne et. a., 2000). Increasing the seed particle concentration led to a continued increase in the yield, along with a decrease in the O/C ratio of the SOA as condensation of less-oxidized products was enhanced. The influence of seed acidity on isoprene SOA yields is well documented (Czoschke, 2003; Surratt et al., 2007; Offenberg et al., 2009), and the magnitude of the SOA yield enhancement in the presence of acidic seeds relative to neutral seeds in our work (factor of 2–3) is similar to these previous studies. Because a systematic isoprene SOA yield enhancement in the presence of neutral seeds (relative to unseeded conditions) is not observed in chamber studies (Chhabra et al.,

2010; Brégonzio-Rozier et al., 2014), these measurements suggest seed particles are required in flow reactor measurements of isoprene SOA (and potentially other types of SOA as well) in order to more closely simulate condensation conditions in environmental chambers.

4 Conclusions

We performed a systematic intercomparison study of the chemistry and yields of SOA generated from OH oxidation of a common set of gas-phase precursors in several environmental chambers and a flow reactor. The most significant experimental parameters that varied between chambers and the flow reactor were OH concentration, residence time, and use of seed particles to promote condensation of oxidized vapors. The OH concentrations were 100 to 1000 times higher in the flow reactor, and residence times were 100 to 400 times higher in the environmental chambers. Within the range of approximate OH exposure overlap of (1–4) $\times 10^{11}$ molec cm^{-3} s, the SOA mass spectra and oxidation state were similar in both systems. The SOA yields for representative systems tracked each other but were lower in the flow reactor, probably in part because chamber SOA experiments were done with seed particles to promote condensation of oxidized vapors. Because SOA composition appears to be governed primarily by gas-phase OH oxidation processes, our results suggest that either flow reactors or chambers are properly characterizing SOA oxidative aging mechanisms representative of ambient conditions. However, SOA yields appear highly sensitive to the relative timescales of gas-phase OH oxidation and condensation processes. Simple calculations and measurements with seed particles suggest that condensation processes may be residence-time-limited in flow reactors depending on the mass accommodation coefficient of the oxidized vapors onto pre-existing particles. This could lead to underestimation of SOA yields. On the other hand, running an environmental chamber or flow reactor under conditions where partitioning is overestimated relative to atmospheric conditions will lead to a corresponding overestimation of SOA yields. Environmental chambers are commonly used to constrain SOA yields at low OH exposures, but flow reactors are needed to constrain SOA yields at higher OH exposures than 1–2 days of equivalent atmospheric oxidation, because environmental chamber SOA yield measurements appear to significantly underestimate atmospheric SOA formation rates when extrapolated over multiple days of equivalent atmospheric oxidation.

Acknowledgements. This work was supported by the Atmospheric Chemistry Program of the National Science Foundation, grants AGS-1244918 and ATM-0854916 to Boston College and AGS-1244999 and AGS-0904292 to Aerodyne Research, Inc., AGS-1244995 to the Pennsylvania State University, AGS-1056225 and AGS-1245011 to the Massachusetts Institute of Technology, and the Office of Science (BER), Department of Energy (Atmospheric Systems Research) grants DE-SC0006980, DE-SC0011935 and DE-FG02-05ER63995 to Boston College and Aerodyne Research, Inc. ATL acknowledges Paola Massoli, Adam Ahern, David Croasdale, Justin Wright, Alex Martin for help with previous experimental studies referenced in this manuscript. PSC acknowl-

edges Xuan Zhang, Christine Loza, and Arthur Chan for help in data analysis of previous chamber studies. We thank the referees and members of Prof. Jose Jimenez' research group at the University of Colorado - Boulder for their additional comments in the interactive discussion of this manuscript.

References

references

Aiken, A., DeCarlo, P., Kroll, J., Worsnop, D., Huffman, J., Docherty, K., Ulbrich, I., Mohr, C., Kimmel, J., and Sueper, D.: O/C and OM/OC ratios of primary, secondary, and ambient organic aerosols with high-resolution time-of-flight aerosol mass spectrometry, Environ. Sci. Technol., 42, 4478–4485, 2008.

Atkinson, R.: Kinetics and mechanisms of the gas-phase reactions of the hydroxyl radical with organic compounds under atmospheric conditions, Chem. Rev., 86, 69–201, 1986.

Bahreini, R., Middlebrook, A. M., Brock, C. A., De Gouw, J. A., Mckeen, S. A., Williams, L. R., Daumit, K. E., Lambe, A. T., Massoli, P., Canagaratna, M. R., Ahmadov, R., Carrasquillo, A. J., Cross, E. S., Ervens, B., Holloway, J. S., Hunter, J. F., Onasch, T. B., Pollack, I. B., Roberts, J. M., Ryerson, T. B., Warneke, C., Davidovits, P., Worsnop, D. R., and Kroll, J. H.: Mass spectral analysis of organic aerosol formed downwind of the Deepwater Horizon oil spill: field studies and laboratory confirmations, Environ. Sci. Technol., 46, 8025–8034, 2012.

Bergström, R., Denier van der Gon, H. A. C., Prévôt, A. S. H., Yttri, K. E., and Simpson, D.: Modelling of organic aerosols over Europe (2002–2007) using a volatility basis set (VBS) framework: application of different assumptions regarding the formation of secondary organic aerosol, Atmos. Chem. Phys., 12, 8499–8527, doi:http://dx.doi.org/10.5194/acp-12-8499-201210.5194/acp-12-8499-2012, 2012.

Bernard, F., Fedioun, I., Peyroux, F. Quilgars, A., Daële, V., and Mellouki, A.: Thresholds of secondary organic aerosol formation by ozonolysis of monoterpenes measured in a laminar flow aerosol reactor, J. Aerosol Sci., 43, 14–30, 2012.

Brégonzio-Rozier, L., Siekmann, F., Giorio, C., Pangui, E., Morales, S. B., Temime-Roussel, B., Gratien, A., Michoud, V., Ravier, S., Tapparo, A., Monod, A., and Doussin, J.-F.: Gaseous products and Secondary Organic Aerosol formation during long term oxidation of isoprene and methacrolein, Atmos. Chem. Phys. Discuss., 14, 22507–22545, doi:http://dx.doi.org/10.5194/acpd-14-22507-201410.5194/acpd-14-22507-2014, 2014.

Canagaratna, M. R., Jimenez, J. L., Kroll, J. H., Chen, Q., Kessler, S. H., Massoli, P., Hildebrandt Ruiz, L., Fortner, E., Williams, L. R., Wilson, K. R., Surratt, J. D., Donahue, N. M., Jayne, J. T., and Worsnop, D. R.: Elemental ratio measurements of organic compounds using aerosol mass spectrometry: characterization, improved calibration, and implications, Atmos. Chem. Phys. Discuss., 14, 19791–19835, doi:http://dx.doi.org/10.5194/acpd-14-19791-201410.5194/acpd-14-19791-2014, 2014.

Cappa, C. D. and Wilson, K. R.: Multi-generation gas-phase oxidation, equilibrium partitioning, and the formation and evolution of secondary organic aerosol, Atmos. Chem. Phys., 12, 9505–9528, doi:http://dx.doi.org/10.5194/acp-12-9505-201210.5194/acp-12-9505-2012, 2012.

Chen, S., Brune, W. H., Lambe, A. T., Davidovits, P., and Onasch, T. B.: Modeling organic aerosol from the oxidation of α-pinene in a Potential Aerosol Mass (PAM) chamber, Atmos. Chem. Phys., 13, 5017–5031, doi:http://dx.doi.org/10.5194/acp-13-5017-201310.5194/acp-13-5017-2013, 2013.

Chhabra, P. S., Flagan, R. C., and Seinfeld, J. H.: Elemental analysis of chamber organic aerosol using an aerodyne high-resolution aerosol mass spectrometer, Atmos. Chem. Phys., 10, 4111–4131, doi:http://dx.doi.org/10.5194/acp-10-4111-201010.5194/acp-10-4111-2010, 2010.

Chhabra, P. S., Ng, N. L., Canagaratna, M. R., Corrigan, A. L., Russell, L. M., Worsnop, D. R., Flagan, R. C., and Seinfeld, J. H.: Elemental composition and oxidation of chamber organic aerosol, Atmos. Chem. Phys., 11, 8827–8845, doi:http://dx.doi.org/10.5194/acp-11-8827-201110.5194/acp-11-8827-2011, 2011.

Czoschke, N.: Effect of acidic seed on biogenic secondary organic aerosol growth, Atmos. Environ., 37, 4287–4299, 2003.

Davis, D. D., Ravishankara, A. R., and Fischer, S.: SO_2 oxidation via the hydroxyl radical: atmospheric fate of HSO_x radicals, Geophys. Res. Lett., 6, 113–116, 1979.

De Gouw, J. A., Middlebrook, A. M., Warneke, C., Ahmadov, R., Atlas, E. L., Bahreini, R., Blake, D. R., Brock, C. A., Brioude, J., Fahey, D. W., Fehsenfeld, F. C., Holloway, J. S., Le Henaff, M., Lueb, R. A., Mckeen, S. A., Meagher, J. F., Murphy, D. M., Paris, C., Parrish, D. D., Perring, A. E., Pollack, I. B., Ravishankara, A. R., Robinson, A. L., Ryerson, T. B., Schwarz, J. P., Spackman, J. R., Srinivasan, A., and Watts, L. A.: Organic aerosol formation downwind from the Deepwater Horizon oil spill, Science, 331, 1295–1299, 2011.

DeCarlo, P. F., Kimmel, J. R., Trimborn, A., Northway, M. J., Jayne, J. T., Aiken, A. C., Gonin, M., Fuhrer, K., Horvath, T., Docherty, K. S., Worsnop, D. R., and Jimenez, J. L.: Field-deployable, high-resolution, time-of-flight aerosol mass spectrometer, Anal. Chem., 78, 8281–8289, 2006.

Drewnick, F., Hings, S., DeCarlo, P., Jayne, J., Gonin, M., Fuhrer, K., Weimer, S., Jimenez, J., Demerjian, K., Borrmann, S., and Worsnop, D.: A new Time-of-Flight Aerosol Mass Spectrometer (TOF-AMS) – instrument description and first field deployment, Aerosol Sci. Tech., 39, 637–658, 2005.

Eddingsaas, N. C., Loza, C. L., Yee, L. D., Chan, M., Schilling, K. A., Chhabra, P. S., Seinfeld, J. H., and Wennberg, P. O.: α-pinene photooxidation under controlled chemical conditions – Part 2: SOA yield and composition in low- and high-NO_x environments, Atmos. Chem. Phys., 12, 7413–7427, doi:http://dx.doi.org/10.5194/acp-12-7413-201210.5194/acp-12-7413-2012, 2012.

Ehn, M., Thornton, J. A., Kleist, E., Sipilä, M., Junninen, H., Pullinen, I., Springer, M., Rubach, F., Tillmann, R., Lee, B., Lopez-Hilfiker, F., Andres, S., Acir, I.-H., Rissanen, M., Jokinen, T., Schobesberger, S., Kangasluoma, J., Kontkanen, J., Nieminen, T., Kurtén, T., Nielsen, L. B., Jørgensen, S., Kjaergaard, H. G., Canagaratna, M., Dal Maso, M., Berndt, T., Petäjä, T., Wahner, A., Kerminen, V.-M., Kulmala, M., Worsnop, D. R., Wildt, J., and Mentel, T. F.: A large source of low-volatility secondary organic aerosol, Nature, 506(7489), 47679, 2014.

Fountoukis, C., Megaritis, A. G., Skyllakou, K., Charalampidis, P. E., Pilinis, C., Denier van der Gon, H. A. C., Crippa, M., Canonaco, F., Mohr, C., Prévôt, A. S. H., Allan, J. D., Poulain, L., Petäjä, T., Tiitta, P., Carbone, S., Kiendler-Scharr, A., Nemitz, E., O'Dowd, C., Swietlicki, E., and Pandis, S. N.: Organic aerosol concentration and composition over Europe: insights from comparison of regional model predictions with aerosol mass spectrometer factor analysis, Atmos. Chem. Phys., 14, 9061–9076, doi:http://dx.doi.org/10.5194/acp-14-9061-201410.5194/acp-14-9061-2014, 2014.

Hall IV, W. A., Pennington, M. R., and Johnston, M. V.: Molecular transformations accompanying the aging of laboratory secondary organic aerosol, Environ. Sci. Technol., 47, 2230–2237, 2013.

Hallquist, M., Wenger, J. C., Baltensperger, U., Rudich, Y., Simpson, D., Claeys, M., Dommen, J., Donahue, N. M., George, C., Goldstein, A. H., Hamilton, J. F., Herrmann, H., Hoffmann, T., Iinuma, Y., Jang, M.,

Jenkin, M. E., Jimenez, J. L., Kiendler-Scharr, A., Maenhaut, W., McFiggans, G., Mentel, Th. F., Monod, A., Prévôt, A. S. H., Seinfeld, J. H., Surratt, J. D., Szmigielski, R., and Wildt, J.: The formation, properties and impact of secondary organic aerosol: current and emerging issues, Atmos. Chem. Phys., 9, 5155–5236, doi:http://dx.doi.org/10.5194/acp-9-5155-200910.5194/acp-9-5155-2009, 2009.

Hamilton, J. F., Rami Alfarra, M., Wyche, K. P., Ward, M. W., Lewis, A. C., McFiggans, G. B., Good, N., Monks, P. S., Carr, T., White, I. R., and Purvis, R. M.: Investigating the use of secondary organic aerosol as seed particles in simulation chamber experiments, Atmos. Chem. Phys., 11, 5917–5929, doi:http://dx.doi.org/10.5194/acp-11-5917-201110.5194/acp-11-5917-2011, 2011.

Heald, C. L., Kroll, J. H., Jimenez, J. L., Docherty, K. S., DeCarlo, P. F., Aiken, A. C., Chen, Q., Martin, S. T., Farmer, D. K., and Artaxo, P.: A simplified description of the evolution of organic aerosol composition in the atmosphere, Geophys. Res. Lett., 37, L08803, doi:http://dx.doi.org/10.1029/2010GL04273710.1029/2010GL042737, 2010.

Henry, K. and Donahue, N.: Photochemical aging of α-pinene secondary organic aerosol: effects of OH radical sources and photolysis, J. Phys. Chem.-US, 116, 5932–5940, 2012.

Hildebrandt, L., Donahue, N. M., and Pandis, S. N.: High formation of secondary organic aerosol from the photo-oxidation of toluene, Atmos. Chem. Phys., 9, 2973–2986, doi:http://dx.doi.org/10.5194/acp-9-2973-200910.5194/acp-9-2973-2009, 2009.

Hunter, J. F., Carrasquillo, A. J., Daumit, K. E., and Kroll, J. H.: Secondary organic aerosol formation from acyclic, monocyclic, and polycyclic alkanes, Environ. Sci. Technol., 48, 10227–10234, 2014.

Jang, M., Carroll, B., Chandramouli, B., and Kamens, R. M., Particle Growth By Acid-Catalyzed Heterogeneous Reactions of Organic Carbonyls on Preexisting Aerosols, Environ. Sci. Technol., 37, 3828–3837, 2003.

Jayne, J. T., Leard, D. C., Zhang, X., Davidovits, P., Smith, K. A., Kolb, C. E., and Worsnop, D. R.: Development of an Aerosol Mass Spectrometer for Size and Composition Analysis of Submicron Particles, Aerosol Sci. Technol., 33, 49–70, 2000.

Jimenez, J. L., Canagaratna, M. R., Donahue, N. M., Prevot, A. S. H., Zhang, Q., Kroll, J. H., DeCarlo, P. F., Allan, J. D., Coe, H., Ng, N. L., Aiken, A. C., Docherty, K. S., Ulbrich, I. M., Grieshop, A. P., Robinson, A. L., Duplissy, J., Smith, J. D., Wilson, K. R., Lanz, V. A., Hueglin, C., Sun, Y. L., Tian, J., Laaksonen, A., Raatikainen, T., Rautiainen, J., Vaattovaara, P., Ehn, M., Kulmala, M., Tomlinson, J. M., Collins, D. R., Cubison, M. J., Dunlea, J., Huffman, J. A., Onasch, T. B., Alfarra, M. R., Williams, P. I., Bower, K., Kondo, Y., Schneider, J., Drewnick, F., Borrmann, S., Weimer, S., Demerjian, K., Salcedo, D., Cottrell, L., Griffin, R., Takami, A., Miyoshi, T., Hatakeyama, S., Shimono, A., Sun, J. Y., Zhang, Y. M., Dzepina, K., Kimmel, J. R., Sueper, D., Jayne, J. T., Herndon, S. C., Trimborn, A. M., Williams, L. R., Wood, E. C., Middlebrook, A. M., Kolb, C. E., Baltensperger, U., and Worsnop, D. R.: Evolution of organic aerosols in the atmosphere, Science, 326, 1525–1529, 2009.

Jo, D. S., Park, R. J., Kim, M. J., and Spracklen, D. V.: Effects of chemical aging on global secondary organic aerosol using the volatility basis set approach, Atmos. Environ., 81, 230–244, 2013.

Kanakidou, M., Seinfeld, J. H., Pandis, S. N., Barnes, I., Dentener, F. J., Facchini, M. C., Van Dingenen, R.,

Ervens, B., Nenes, A., Nielsen, C. J., Swietlicki, E., Putaud, J. P., Balkanski, Y., Fuzzi, S., Horth, J., Moortgat, G. K., Winterhalter, R., Myhre, C. E. L., Tsigaridis, K., Vignati, E., Stephanou, E. G., and Wilson, J.: Organic aerosol and global climate modelling: a review, Atmos. Chem. Phys., 5, 1053–1123, doi:http://dx.doi.org/10.5194/acp-5-1053-200510.5194/acp-5-1053-2005, 2005.

Kang, E., Root, M. J., Toohey, D. W., and Brune, W. H.: Introducing the concept of Potential Aerosol Mass (PAM), Atmos. Chem. Phys., 7, 5727–5744, doi:http://dx.doi.org/10.5194/acp-7-5727-200710.5194/acp-7-5727-2007, 2007.

Kang, E., Toohey, D. W., and Brune, W. H.: Dependence of SOA oxidation on organic aerosol mass concentration and OH exposure: experimental PAM chamber studies, Atmos. Chem. Phys., 11, 1837–1852, doi:http://dx.doi.org/10.5194/acp-11-1837-201110.5194/acp-11-1837-2011, 2011.

Keller, A. and Burtscher, H.: A continuous photo-oxidation flow reactor for a defined measurement of the SOA formation potential of wood burning emissions, J. Aerosol Sci., 49, 9–20, 2012.

Kroll, J., Ng, N., Murphy, S., Flagan, R., and Seinfeld, J.: Secondary organic aerosol formation from isoprene photooxidation, Environ. Sci. Technol., 40, 1869–1877, 2006.

Kroll, J. H., Donahue, N. M., Jimenez, J. L., Kessler, S. H., Canagaratna, M. R., Wilson, K. R., Altieri, K. E., Mazzoleni, L. R., Wozniak, A. S., Bluhm, H., Mysak, E. R., Smith, J. D., Kolb, C. E., and Worsnop, D. R.: Carbon oxidation state as a metric for describing the chemistry of atmospheric organic aerosol, Nature Chemistry, 3, 133–139, 2011.

Lambe, A. T., Ahern, A. T., Williams, L. R., Slowik, J. G., Wong, J. P. S., Abbatt, J. P. D., Brune, W. H., Ng, N. L., Wright, J. P., Croasdale, D. R., Worsnop, D. R., Davidovits, P., and Onasch, T. B.: Characterization of aerosol photooxidation flow reactors: heterogeneous oxidation, secondary organic aerosol formation and cloud condensation nuclei activity measurements, Atmos. Meas. Tech., 4, 445–461, doi:http://dx.doi.org/10.5194/amt-4-445-201110.5194/amt-4-445-2011, 2011a.

Lambe, A. T., Onasch, T. B., Massoli, P., Croasdale, D. R., Wright, J. P., Ahern, A. T., Williams, L. R., Worsnop, D. R., Brune, W. H., and Davidovits, P.: Laboratory studies of the chemical composition and cloud condensation nuclei (CCN) activity of secondary organic aerosol (SOA) and oxidized primary organic aerosol (OPOA), Atmos. Chem. Phys., 11, 8913–8928, doi:http://dx.doi.org/10.5194/acp-11-8913-201110.5194/acp-11-8913-2011, 2011b.

Lambe, A. T., Onasch, T. B., Croasdale, D. R., Wright, J. P., Martin, A. T., Franklin, J. P., Massoli, P., Kroll, J. H., Canagaratna, M. R., Brune, W. H., Worsnop, D. R., and Davidovits, P.: Transitions from functionalization to fragmentation reactions of laboratory Secondary Organic Aerosol (SOA) generated from the OH oxidation of alkane precursors, Environ. Sci. Technol., 46, 5430–5437, 2012.

Lambe, A. T., Cappa, C. D., Massoli, P., Onasch, T. B., Forestieri, S. D., Martin, A. T., Cummings, M. J., Croasdale, D. R., Brune, W. H., Worsnop, D. R., and Davidovits, P.: Relationship between oxidation level and optical properties of secondary organic aerosol, Environ. Sci. Technol., 46, 5430–5437, 2013.

Levin, E. J. T., Prenni, A. J., Palm, B. B., Day, D. A., Campuzano-Jost, P., Winkler, P. M., Kreidenweis, S. M., DeMott, P. J., Jimenez, J. L., and Smith, J. N.: Size-resolved aerosol composition and its link to hygroscopicity at a forested site in Colorado, Atmos. Chem. Phys., 14, 2657–2667, doi:http://dx.doi.org/10.5194/acp-14-2657-201410.5194/acp-14-2657-2014, 2014.

Li, Y. P., Elbern, H., Lu, K. D., Friese, E., Kiendler-Scharr, A., Mentel, Th. F., Wang, X. S., Wahner, A., and

Zhang, Y. H.: Updated aerosol module and its application to simulate secondary organic aerosols during IMPACT campaign May 2008, Atmos. Chem. Phys., 13, 6289–6304, doi:http://dx.doi.org/10.5194/acp-13-6289-201310.5194/acp-13-6289-2013, 2013.

Li, R., Palm, B. B., Ortega, A. M., Hlywiak, J., Hu, W., Peng, Z., Day, D. A., Knote, C., Brune, W. H., de Gouw, J. A., Jimenez, J. L.: Modeling the radical chemistry in an Oxidation Flow Reactor: radical formation and recycling, sensitivities, and OH exposure calibration equation, J. Phys. Chem. A., submitted.

Loza, C. L., Chhabra, P. S., Yee, L. D., Craven, J. S., Flagan, R. C., and Seinfeld, J. H.: Chemical aging of *m*-xylene secondary organic aerosol: laboratory chamber study, Atmos. Chem. Phys., 12, 151–167, doi:http://dx.doi.org/10.5194/acp-12-151-201210.5194/acp-12-151-2012, 2012.

Loza, C. L., Craven, J. S., Yee, L. D., Coggon, M. M., Schwantes, R. H., Shiraiwa, M., Zhang, X., Schilling, K. A., Ng, N. L., Canagaratna, M. R., Ziemann, P. J., Flagan, R. C., and Seinfeld, J. H.: Secondary organic aerosol yields of 12-carbon alkanes, Atmos. Chem. Phys., 14, 1423–1439, doi:http://dx.doi.org/10.5194/acp-14-1423-201410.5194/acp-14-1423-2014, 2014.

Mao, J., Ren, X., Brune, W. H., Olson, J. R., Crawford, J. H., Fried, A., Huey, L. G., Cohen, R. C., Heikes, B., Singh, H. B., Blake, D. R., Sachse, G. W., Diskin, G. S., Hall, S. R., and Shetter, R. E.: Airborne measurement of OH reactivity during INTEX-B, Atmos. Chem. Phys., 9, 163–173, doi:http://dx.doi.org/10.5194/acp-9-163-200910.5194/acp-9-163-2009, 2009.

Marcolli., C., Canagaratna, M. R., Worsnop, D. R., Bahreini, R., de Gouw, J. A., Warneke, C., Goldan, P. D., Kuster, W. C., Williams, E. J., Lerner, B. M., Roberts, J. M., Meagher, J. F., Fehsenfeld, F. C., Marchewka, M., Bertman, S. B., and Middlebrook, A. M.: Cluster Analysis of the Organic Peaks in Bulk Mass Spectra Obtained During the 2002 New England Air Quality Study with an Aerodyne Aerosol Mass Spectrometer, Atmos. Chem. Phys., 6, 5649666, doi:http://dx.doi.org/10.5194/acp-6-5649-200610.5194/acp-6-5649-2006, 2006.

Massoli, P., Lambe, A. T., Ahern, A. T., Williams, L. R., Ehn, M., Mikkilä, J., Canagaratna, M. R., Brune, W. H., Onasch, T. B., Jayne, J. T., Petäjä, T., Kulmala, M., Laaksonen, A., Kolb, C. E., Davidovits, P., and Worsnop, D. R.: Relationship between aerosol oxidation level and hygroscopic properties of laboratory generated secondary organic aerosol (SOA) particles, Geophys. Res. Lett., 37, L24801, doi:http://dx.doi.org/10.1029/2010GL04525810.1029/2010GL045258, 2010.

Matsunaga, A. and Ziemann, P.: Gas-wall partitioning of organic compounds in a teflon film chamber and potential effects on reaction product and aerosol yield measurements, Aerosol Sci. Tech., 44, 881–892, 2010.

Mei, F., Setyan, A., Zhang, Q., and Wang, J.: CCN activity of organic aerosols observed downwind of urban emissions during CARES, Atmos. Chem. Phys., 13, 12155–12169, doi:http://dx.doi.org/10.5194/acp-13-12155-201310.5194/acp-13-12155-2013, 2013.

Moore, R., Raatikainen, T., Langridge, J., Bahreini, R., Brock, C., Holloway, J., Lack, D., Middlebrook, A., Perring, A., Schwarz, J., Spackman, J., and Nenes, A.: CCN spectra, hygroscopicity, and droplet activation kinetics of secondary organic aerosol resulting from the 2010 Deepwater Horizon oil spill, Environ. Sci. Technol., 46, 3093–3100, 2012.

Murphy, D. M., Middlebrook, A. M., and Warshawsky, M.: Cluster Analysis of Data from the Particle Analysis by Laser Mass Spectrometry (PALMS) Instrument, Aerosol Sci. Tech., 37, 382–391, 2003.

Ng, N. L., Chhabra, P. S., Chan, A. W. H., Surratt, J. D., Kroll, J. H., Kwan, A. J., McCabe, D. C., Wennberg, P. O., Sorooshian, A., Murphy, S. M., Dalleska, N. F., Flagan, R. C., and Seinfeld, J. H.: Effect of NO_x level on secondary organic aerosol (SOA) formation from the photooxidation of terpenes, Atmos. Chem. Phys., 7, 5159–5174, doi:http://dx.doi.org/10.5194/acp-7-5159-200710.5194/acp-7-5159-2007, 2007.

Ng, N. L., Canagaratna, M. R., Zhang, Q., Jimenez, J. L., Tian, J., Ulbrich, I. M., Kroll, J. H., Docherty, K. S., Chhabra, P. S., Bahreini, R., Murphy, S. M., Seinfeld, J. H., Hildebrandt, L., Donahue, N. M., DeCarlo, P. F., Lanz, V. A., Prévôt, A. S. H., Dinar, E., Rudich, Y., and Worsnop, D. R.: Organic aerosol components observed in Northern Hemispheric datasets from Aerosol Mass Spectrometry, Atmos. Chem. Phys., 10, 4625–4641, doi:http://dx.doi.org/10.5194/acp-10-4625-201010.5194/acp-10-4625-2010, 2010.

Offenberg, J., Lewandowski, M., Edney, E., Kleindienst, T., and Jaoui, M.: Influence of aerosol acidity on the formation of secondary organic aerosol from biogenic precursor hydrocarbons, Environ. Sci. Technol., 43, 7742–7747, 2009.

Ofner, J., Krüger, H.-U., and Zetzsch, C.: Time Resolved Infrared Spectroscopy of Formation and Processing of Secondary Organic Aerosol, Z. Phys. Chem., 224, 1171183, 2010.

Ortega, A. M., Day, D. A., Cubison, M. J., Brune, W. H., Bon, D., de Gouw, J. A., and Jimenez, J. L.: Secondary organic aerosol formation and primary organic aerosol oxidation from biomass-burning smoke in a flow reactor during FLAME-3, Atmos. Chem. Phys., 13, 11551–11571, doi:http://dx.doi.org/10.5194/acp-13-11551-201310.5194/acp-13-11551-2013, 2013.

Pfaffenberger, L., Barmet, P., Slowik, J. G., Praplan, A. P., Dommen, J., Prévôt, A. S. H., and Baltensperger, U.: The link between organic aerosol mass loading and degree of oxygenation: an α-pinene photooxidation study, Atmos. Chem. Phys., 13, 6493–6506, doi:http://dx.doi.org/10.5194/acp-13-6493-201310.5194/acp-13-6493-2013, 2013.

Pierce, J. R., Engelhart, G. J., Hildebrandt, L., Weitkamp, E. A., Pathak, R. K., Donahue, N. M., Robinson, A. L., Adams, P. J., and Pandis, S. N.: Constraining particle evolution from wall losses, coagulation, and condensation-evaporation in smog-chamber experiments: optimal estimation based on size distribution measurements, Aerosol Sci. Tech., 42, 1001–1015, 2008.

Presto, A. and Donahue, N.: Investigation of α-pinene+ ozone secondary organic aerosol formation at low total aerosol mass, Environ. Sci. Technol., 40, 3536–3543, 2006.

Presto, A., Hartz, K., and Donahue, N.: Secondary organic aerosol production from terpene ozonolysis. 2. Effect of NO_x concentration, Environ. Sci. Technol., 39, 7046–7054, 2005.

Renbaum, L. H. and Smith, G. D.: Artifacts in measuring aerosol uptake kinetics: the roles of time, concentration and adsorption, Atmos. Chem. Phys., 11, 6881–6893, doi:http://dx.doi.org/10.5194/acp-11-6881-201110.5194/acp-11-6881-2011, 2011.

Saleh, R., Donahue, N. M., and Robinson, A. L.: Time scales for gas-particle partitioning equilibration of secondary organic aerosol formed from α-pinene ozonolysis, Environ. Sci. Technol., 47, 5588–5594, 2013.

Seinfeld, J. H., and Pandis, S. N.: Atmospheric Chemistry and Physics: From Air Pollution to Climate Change, 2nd edition, J. Wiley, New York, 2006.

Shrivastava, M., Fast, J., Easter, R., Gustafson Jr., W. I., Zaveri, R. A., Jimenez, J. L., Saide, P., and Hodzic, A.: Modeling organic aerosols in a megacity: comparison of simple and complex representations of the volatility basis set approach, Atmos. Chem. Phys., 11, 6639–6662, doi:http://dx.doi.org/10.5194/acp-11-6639-201110.5194/acp-11-6639-2011, 2011.

Sihto, S.-L., Mikkilä, J., Vanhanen, J., Ehn, M., Liao, L., Lehtipalo, K., Aalto, P. P., Duplissy, J., Petäjä, T., Kerminen, V.-M., Boy, M., and Kulmala, M.: Seasonal variation of CCN concentrations and aerosol activation properties in boreal forest, Atmos. Chem. Phys., 11, 13269–13285, doi:http://dx.doi.org/10.5194/acp-11-13269-201110.5194/acp-11-13269-2011, 2011.

Slowik, J. G., Wong, J. P. S., and Abbatt, J. P. D.: Real-time, controlled OH-initiated oxidation of biogenic secondary organic aerosol, Atmos. Chem. Phys., 12, 9775–9790, doi:http://dx.doi.org/10.5194/acp-12-9775-201210.5194/acp-12-9775-2012, 2012.

Spracklen, D. V., Jimenez, J. L., Carslaw, K. S., Worsnop, D. R., Evans, M. J., Mann, G. W., Zhang, Q., Canagaratna, M. R., Allan, J., Coe, H., McFiggans, G., Rap, A., and Forster, P.: Aerosol mass spectrometer constraint on the global secondary organic aerosol budget, Atmos. Chem. Phys., 11, 12109–12136, doi:http://dx.doi.org/10.5194/acp-11-12109-201110.5194/acp-11-12109-2011, 2011.

Surratt, J. D., Lewandowski, M., Offenberg, J. H., Jaoui, M., Kleindienst, T. E., Edney, E. O., and Seinfeld, J. H.: Effect of acidity on secondary organic aerosol formation from isoprene, Environ. Sci. Technol., 41, 5363–5369, 2007.

Tkacik, D., Presto, A., Donahue, N., and Robinson, A.: Secondary organic aerosol formation from intermediate-volatility organic compounds: cyclic, linear, and branched alkanes, Environ. Sci. Technol., 46, 8773–8781, 2012.

Volkamer, R., Ziemann, P. J., and Molina, M. J.: Secondary Organic Aerosol Formation from Acetylene (C_2H_2): seed effect on SOA yields due to organic photochemistry in the aerosol aqueous phase, Atmos. Chem. Phys., 9, 1907–1928, doi:http://dx.doi.org/10.5194/acp-9-1907-200910.5194/acp-9-1907-2009, 2009.

Wang, B., Lambe, A., Massoli, P., Onasch, T. B., Davidovits, P., Worsnop, D. R., and Knopf, D. A.: The deposition ice nucleation and immersion freezing potential of amorphous secondary organic aerosol: pathways for ice and mixed-phase cloud formation, J. Geophys. Res., 117, D16209, doi:http://dx.doi.org/10.1029/2012JD01806310.1029/2012JD018063, 2012.

Wong, J. P. S., Lee, A. K. Y., Slowik, J. G., Cziczo, D. J., Leaitch, W. R., Macdonald, A., and Abbatt, J. P. D.: Oxidation of ambient biogenic secondary organic aerosol by hydroxyl radicals: effects on cloud condensation nuclei activity, Geophys. Res. Lett., 38, L22805, doi:http://dx.doi.org/10.1029/2011GL04935110.1029/2011GL049351, 2011.

Zhang, Q., Alfarra, M., Worsnop, D., Allan, J., Coe, H., Canagaratna, M., and Jimenez, J.: Deconvolution and quantification of hydrocarbon-like and oxygenated organic aerosols based on aerosol mass spectrometry, Environ. Sci. Technol., 39, 4938–4952, 2005.

Zhang, Q., Jimenez, J. L., Canagaratna, M. R., Allan, J. D., Coe, H., Ulbrich, I., Alfarra, M. R., Takami, A., Middlebrook, A. M., Sun, Y. L., Dzepina, K., Dunlea, E., Docherty, K., DeCarlo, P. F., Salcedo, D., Onasch, T.,

Jayne, J. T., Miyoshi, T., Shimono, A., Hatakeyama, S., Takegawa, N., Kondo, Y., Schneider, J., Drewnick, F., Borrmann, S., Weimer, S., Demerjian, K., Williams, P., Bower, K., Bahreini, R., Cottrell, L., Griffin, R. J., Rautiainen, J., Sun, J. Y., Zhang, Y. M., and Worsnop, D. R.: Ubiquity and dominance of oxygenated species in organic aerosols in anthropogenically-influenced Northern Hemisphere midlatitudes, Geophys. Res. Lett., 34, L13801, doi:http://dx.doi.org/10.1029/2007GL02997910.1029/2007GL029979, 2007.

Zhang, X., Lin, Y.-H., Surratt, J. D., Zotter, P, Prévôt, A. S. H., and Weber, R. J.: Light-absorbing soluble organic aerosol in Los Angeles and Atlanta: a contrast in secondary organic aerosol, Geophys. Res. Lett., 38, L21810, doi:http://dx.doi.org/10.1029/2011GL04938510.1029/2011GL049385, 2011.

Zhang, X., Cappa, C. D., Jathar, S. H., McVay, R. C., Ensberg, J. J., Kleeman, M. J., and Seinfeld, J. H.: Influence of vapor wall loss in laboratory chambers on yields of secondary organic aerosol, P. Natl. Acad. Sci. USA, 111, 5802–5807, 2014.

Table 1. Summary of PAM reactor and environmental chamber OH exposure conditions.

table

Precursor	PAM	Caltech	MIT	PSI	CMU	Refs
isoprene	1.6×10^{11}–1.0×10^{12}	9.5×10^{10}	–	–	–	1–3, 8
α-pinene	2.0×10^{10}–2.2×10^{12}	5.4×10^{10}–1.3×10^{11}	–	9.0×10^{10}–4.0×10^{11}	–	1–4, 7–8, 10
toluene	1.6×10^{11}–2.1×10^{12}	1.5×10^{11}	–	–	–	1–3, 8
m-xylene	4.1×10^{10}–2.1×10^{12}	7.7×10^{10}–1.6×10^{11}	–	–	–	1–3, 7–8
naphthalene	1.6×10^{11}–2.1×10^{12}	2.3×10^{11}	–	–	–	2–3, 8, 10
n-C_{10}	1.6×10^{11}–2.1×10^{12}	–	2.6×10^{11}	–	–	1, 5, 9
cyclodecane	1.6×10^{11}–1.9×10^{12}	–	1.8×10^{11}	–	2.2×10^{10}	1, 5–6
JP-10	1.3×10^{11}–2.0×10^{12}	–	3.3×10^{11}–5.8×10^{11}	–	–	5, 9–10

References: [1] this work; [2] Chhabra et al. (2010); [3] Chhabra et al. (2011); [4] Pfaffenberger et al. (2013); [5] Hunter et al. (2014); [6] Tkacik et al. (2012); [7] Lambe et al. (2011a); [8] Lambe et al. (2011b); [9] Lambe et al. (2012); [10] Lambe et al. (2013).

Table 2. Experimental conditions for PAM reactor, Caltech chamber, and MIT chamber yield measurements shown in Figs. 5–7.

	seed concentration ($\mu g\,m^{-3}$)	maximum [NO_x] added (ppb)	[isoprene] (ppb)	[α-pinene] (ppb)	[JP-10] (ppb)	Refs
Caltech chamber	0–29[a]	0	49–91	13.8–52.4	–	1–3
MIT chamber	50–100[a]	475	–	–	42.9	4
PAM flow reactor	0–59[a]; 0–114[b]	0	462	41–100	55	5–7

[a] ammonium sulfate seed;

[b] sulfuric acid seed;

[1] Chhabra et al. (2010); [2] Ng et al. (2007); [3] Eddingsaas et al. (2012); [4] Hunter et al. (2014); [5] this work; [6] Lambe et al. (2012); [7] Chen et al. (2013).

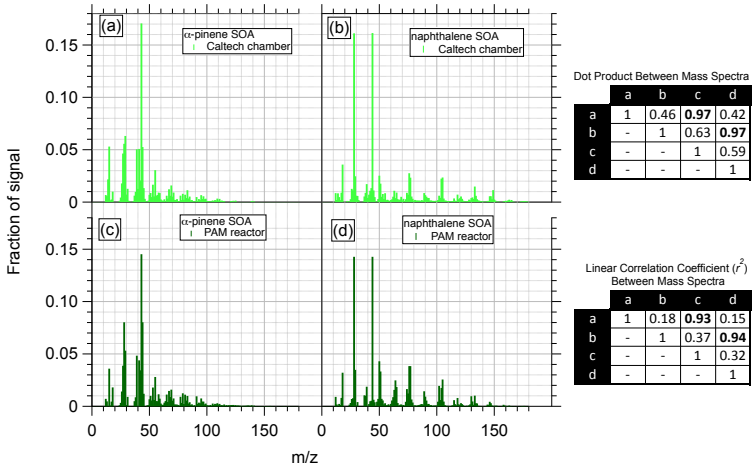

Fig. 1. Aerodyne ToF-AMS spectra of SOA generated in the (**a** and **b**) Caltech environmental chamber and (**c** and **d**) PAM flow reactor from the OH oxidation of α-pinene and naphthalene. Caltech chamber data obtained from Chhabra et al. (2011).

figure

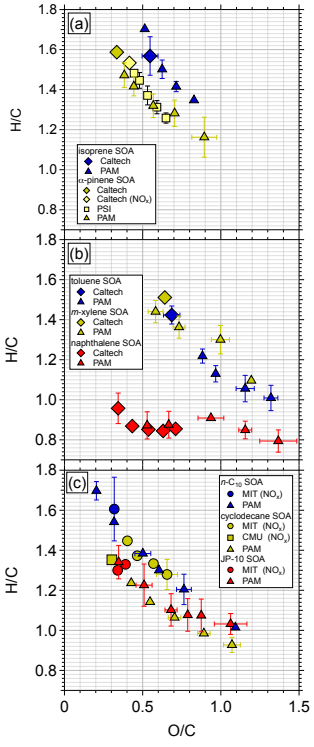

Fig. 2. Van Krevelen diagrams showing $\mathrm{H/C}$ ratio as a function of $\mathrm{O/C}$ ratio for SOA generated in the PAM flow reactor and environmental chambers by OH oxidation of **(a)** biogenic, **(b)** aromatic and **(c)** alkane precursors. Error bars indicate $\pm 1\sigma$ uncertainty in binned $\mathrm{O/C}$ and $\mathrm{H/C}$ ratio measurements. Caltech, PSI, CMU, and MIT chamber data obtained from Chhabra et al. (2011); Pfaffenberger et al. (2013) (binned averages of $\mathrm{O/C}$ and $\mathrm{H/C}$ data from experiments # 1–9), Tkacik et al. (2012), and Hunter et al. (2014) respectively.

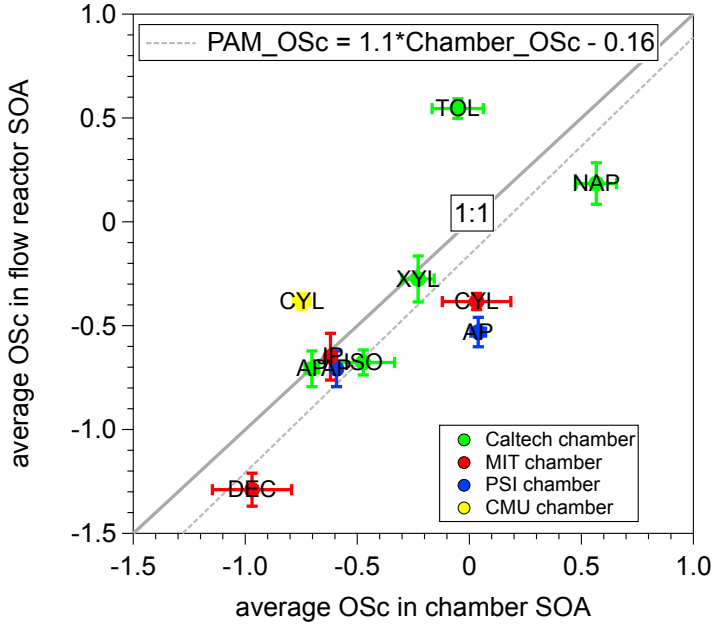

Fig. 3. Average carbon oxidation state ($\overline{\mathrm{OSc}}$; $\overline{\mathrm{OSc}} \approx 2 \times \mathrm{O/C} - \mathrm{H/C}$) of flow reactor- and environmental chamber-generated SOA. Error bars indicate $\pm 1\sigma$ uncertainty in binned $\overline{\mathrm{OSc}}$ measurements. Markers indicate SOA precursor: TOL = toluene; NAP = naphthalene; XYL = m-xylene; CYL = cyclodecane; JP = JP-10; ISO = isoprene; AP = α-pinene; DEC = n-C_{10}. Caltech, PSI, CMU, and MIT chamber data obtained from Chhabra et al. (2011); Pfaffenberger et al. (2013); Tkacik et al. (2012), and Hunter et al. (2014) respectively.

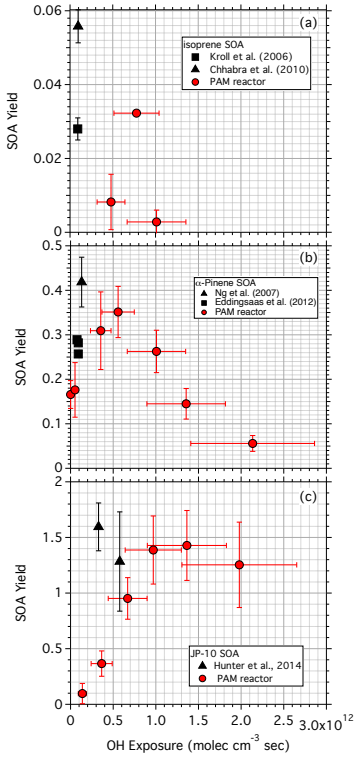

Fig. 4. Yields of SOA produced from photoxidation of **(a)** isoprene, **(b)** α-pinene, and **(c)** tetracyclo[5.2.1.$0^{2,6}$]decane (JP-10) in environmental chambers and PAM reactor as a function of OH exposure. The OH exposure in (c is corrected for reductions in OH levels upon JP-10 addition (see Section 2.1). Error bars indicate $\pm 1\sigma$ uncertainty in binned SOA yield measurements and 34% uncertainty in OH exposure values (Li et. al., 2015). Black markers indicate data from Kroll et al. (2006); Chhabra et al. (2010); Eddingsaas et al. (2012), and Ng et al. (2007) obtained in the Caltech chamber and data from Hunter et al. (2014) ~~was~~ obtained in the MIT chamber.

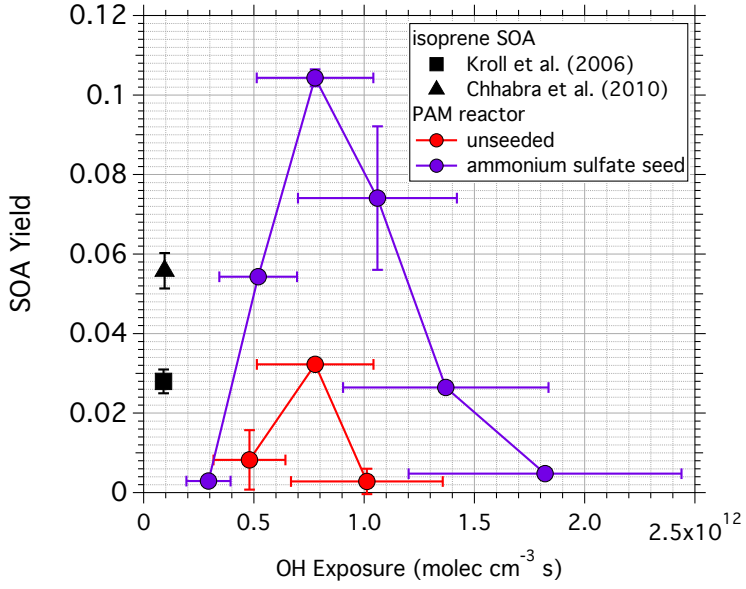

Fig. 5. Yields of SOA produced from photoxidation of isoprene in the PAM reactor as a function of OH exposure in the presence of $20\,\mu g\,m^{-3}$ ammonium sulfate seed. Error bars indicate $\pm 1\sigma$ uncertainty in binned SOA yield measurements and 34% uncertainty in OH exposure values (Li et. al., 2015).

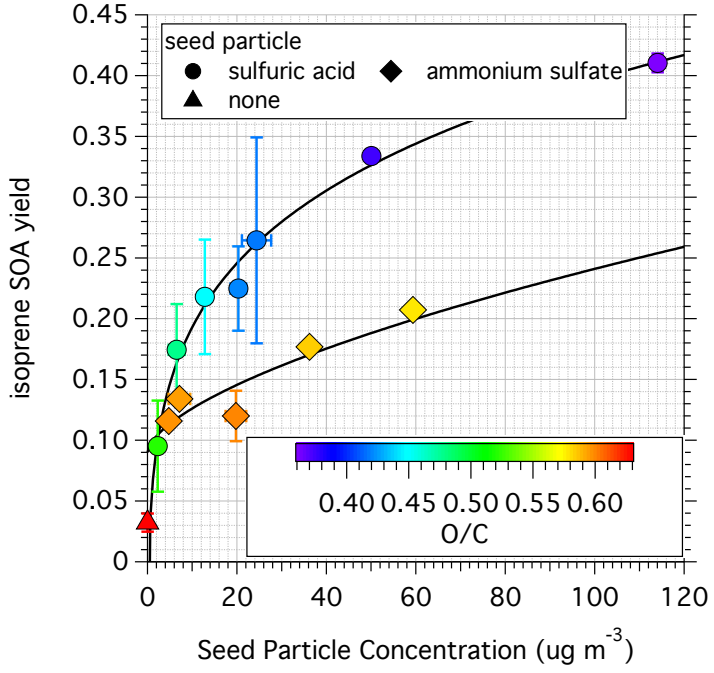

Fig. 6. Yields of isoprene SOA produced in the PAM reactor at an OH exposure of $7.8 \times 10^{11}\,\mathrm{molec\,cm^{-3}\,s}$ as a function of seed particle concentration using ammonium sulfate and sulfuric acid seeds. Error bars indicate $\pm 1\sigma$ uncertainty in binned measurements. Lines are power law fits to guide the eye.